fibroblasts, thereby negatively regulating the expression of MMP gene in autocrine and paracrine fashion. In this regard, it should be pointed out that the addition of exogenous OPN down-regulated the MMP-13 expression in cultured tendon fibroblasts of WT mice. Similarly, the addition of OPN to cultured tendon fibroblast of OPN-deficient mice resulted in the down-regulation of MMP-13 expression. Thus, we favored the scenario in which a sharp reduction of OPN expression at day 5 after stress deprivation played a critical role in the subsequent induction of MMP-13 expression. We reasoned that the reduction of OPN expression in tendon tissue of WT mice made it difficult to maintain the interaction between tendon fibroblasts and OPN *in situ*, thus inevitably resulting in the abrogation of interaction between OPN and its receptor on fibroblasts. To mimic this environment, we added synthetic peptide GRGDS, which interferes with the interaction of OPN with its receptor, to the cultured fibroblasts of WT mice and found that MMP-13 expression was significantly up-regulated, however, control peptide GRGES was without effect. In accordance with our results, it was previously reported that IL-1 stimulated MMP-2 expression in cultured cardiac fibroblasts and this stimulation was significantly reduced by OPN. Importantly, the OPN effect was abrogated by an integrin antagonist, indicating that OPN's interaction with its receptor inhibited IL-1-stimulated MMP expression (Xie et al., 2003). We further demonstrated that the anti-αv integrin antibody, which also interferes with the binding of OPN to its αvβ3 integrin receptor, also significantly augmented MMP-13 expression when added to the cultured tendon fibroblasts of WT mice. One may argue that anti-integrin antibodies and antagonistic peptides may activate integrins (Carron et al., 2000; D'Alonzo et al., 2002; Humphries et al., 2005). Therefore, we attempted to inhibit the interaction of OPN and its receptor by using anti-OPN antibodies. We found that anti-OPN antibody (M5), which interferes with the binding to integrin, but not the control antibody (M3), up-regulate MMP-13 expression. It should be reminded that OPN can be specifically recognized by numbers of cell surface receptors including CD44, RGD-recognizing integrins such as α5β1 and αvβ3 and non-RGD-recognizing integrins such as α4β1 and α9β1 (Weber et al., 1996; Uede et al., 1997; Katagiri et al., 1999; Yamamoto et al., 2003; Diao et al., 2004). Other MMPs might be involved in this remodeling process after stress deprivation. The lack of OPN interaction with its receptor, due to the decreased OPN protein expression by anti-sense OPN, led to the increased MMP-2 expression in mammary epithelial cells (Ronziere et al., 2005). However, we found that MMP-2 expression did not differ in the absence or presence of OPN during the course of tendon tissue remodeling.

One critical issue that should be discussed here is the rationale why the level of MMP-13 expression in cultured fibroblasts of OPN-deficient mice was not significantly higher as compared to those of wild-type fibroblasts if OPN negatively regulated MMP-13 expression. It is possible that cultured fibroblasts of OPN-deficient mice was stimulated by OPN in calf serum in culture, although we changed the culture condition to serum-starved condition prior to MMP-13 assay. In accordance with this hypothesis, MMP-13 expression in cultured fibroblasts of OPN-deficient mice was further down-regulated by the addition of exogenous OPN. Nevertheless, the abrogation of this interaction by M5 antibody, significantly up-regulated MMP-13 expression in cultured fibroblasts of OPN-deficient mice. More importantly, *in vivo* MMP-13 expression was up-regulated in tendon of OPN-deficient mice at day 14 after denervation-induced stress deprivation, although this up-regulation was considerably low as compared to those in WT mice. Taken together, these data suggest that the reduction of OPN expression, thus abrogation of pre-existing interaction between OPN and tendon fibroblasts may play a key role during tendon remodeling by regulating MMP-13 expression.

Osteopontin could also suppress collagen synthesis or induce fibroblast apoptosis, thereby modulating remodeling process. We demonstrated that collagen synthesis as defined by type I collagen gene expression was significantly reduced in tendon after stress deprivation. However, importantly, the collagen synthesis did not differ significantly between stress deprived tendon and contralateral loaded tendon, indicating that suppression of collagen synthesis may not account for the decrease in collagen fibril diameter after stress deprivation. We were also unable to detect apoptotic cells during the course of tendon remodeling.

Based on these results, we postulate the following scenario for tendon remodeling caused by denervation-induced mechanical stress deprivation. Stress deprivation of the tendon initiates a dynamic change of OPN expression in fibroblasts, which induces MMP-13 gene expression, resulting in the degradation of the tendon ECM. Thus in tendon remodeling, OPN may act as a transducer of the mechanical stress to the tendon fibroblasts (Denhardt et al., 2001a). It is therefore possible to control the remodeling process of musculoskeletal soft tissues by manipulating OPN local expression or interfering in the interaction of OPN with its receptor.

4. Experimental procedures

4.1. Animals

Osteopontin-deficient ($OPN^{-/-}$) mice were generated according to the previous study (Rittling et al., 1998). Six-week-old male $OPN^{-/-}$ mice backcrossed 9 times to C57BL/6 mice and age-matched B6 male WT mice were used in the experiments. The animal experiments were carried out in the Institute of Animal Experimentation, Hokkaido University School of Medicine, under the Rules and Regulations of the Animal Care and Use Committee, Hokkaido University School of Medicine.

4.2. Real-time quantitative RT-PCR analysis of OPN, MMP, and type I collagen transcript expression

To examine the change of OPN mRNA expression during the course of tissue remodeling, the patellar tendons from the stress deprived right knee in WT mice were removed at days 0, 1, 3, 5, 7, 14, and 42 after surgery. Similarly, the patellar tendons from the control left knee in WT mice were removed at days 0, 3, 7,

14, and 21. To clarify the alteration of MMP-2, -13, and Type I collagen mRNA, the patellar tendons from bilateral knees in WT mice were removed at days 0, 3, 7, 14, and 21 after surgery. Total RNAs were prepared from patellar tendons, and first-strand cDNA was generated with a First-strand cDNA synthesis kit (Amersham Biosciences, Uppsala, Sweden). Real-time quantitative RT-PCR was performed on LightCycler-FastStart DNA Master SYBR Green 1 Systems (Roche Diagnostics, Basel, Switzerland). The specific primers used in this study were as follows: the sense primer for OPN was 5′-ACGACCATGA GATTGGCAGTG-3′ and the anti-sense primer was 5′-TTAG TTGACCTCAGAAGATGA-3′. The sense primer for MMP-2 was 5′-AGATCTTCTTCTTCAAGGACCGGTT-3′ and the anti-sense primer was 5′-GGCTGGTCAGTGGCTTGGGG TA-3′. The sense primer for MMP-13 was 5′-CATCCATCCC GTGACCTTAT-3′ and the anti-sense primer was 5′-GCATG ACTCTCACAATGCGA-3′. The sense primer for Type I collagen was 5′-TTTGTGGACCTCCGGCTC-3′ and the anti-sense primer was 5′-AAGCAGAGCACTCGCCCT-3′. The sense primer for G3PDH was 5′-ACCACAGTCCATGCCAT CAC-3′ and the anti-sense primer was 5′-TCCACCACCCTG TTGCTGTA-3′.

Values in gene expression level of OPN, MMPs, and type I collagen were normalized to those of G3PDH in each tendon sample. For kinetics of gene expression values at day 0 (before surgery) are expressed as 1. The preliminary study indicated that G3PDH gene expression levels were not altered after denervation.

4.3. Immunohistochemistry

Four-micrometer-sections of formalin-fixed and paraffin-embedded mouse tendon tissues were made and deparaffined in xylene, treated with 0.3% hydrogen peroxidase to block endogeneous peroxidase activity. For OPN staining, these sections were then stained with anti-mouse OPN rabbit IgG (O-17; IBL, Gunma, Japan), followed by a DAKO EnVision+ system (DAKO, Carpinteria, CA) as specified by the manufacturers. For macrophage staining, the sections were stained with anti-macrophage rat monoclonal, F4/80 antibody (Serotec Ltd, Oxford, UK) and then biotinylated anti-rat IgG (H+L) (Vector Laboratories, Inc., Burlingame, CA). After washing, the sections were treated with ABC complex (Vector Laboratories, Inc.). Positive staining was visualized by the peroxidase-diaminobenzidine (DAKO, Carpinteria, CA) reaction and the sections were counterstained with Meyer's hematoxylin.

4.4. Terminal deoxynucleotidyltransferase-mediated dUTP end labeling (TUNEL)

TUNEL assay was conducted by using an *in situ* Apoptosis Detection Kit according to the manufacturer's instruction (Takara Bio Inc., Otsu, Japan). Briefly, the sections were incubated with 15 μg/ml proteinase K for 15 min at room temperature and then washed with PBS. Endogenous peroxidase was inactivated by 3% H_2O_2 for 5 min at room temperature and then washed with PBS. Multiple fragmented 3′-OH ends in the sections were labeled with digoxigenin-dUTP in the presence of terminal deoxynucleotidyltransferase (TdT) in a humid atmosphere at 37 °C for 90 min, and then washed with PBS. Peroxidase-conjugated anti-digoxigenin antibody was then reacted with the sections at room temperature for 30 min. Apoptotic nuclei were visualized using the peroxidase-DAB reaction. The sections were then counterstained with methyl green. TUNEL-positive cells in the sections were counted under a light microscope (×200).

4.5. OPN protein secretion

To determine the secretion of OPN protein from tendon fibroblasts, OPN protein levels in culture supernatant were measured with an OPN ELISA kit (Kon et al., 2000) according to the manufacturer's instructions (IBL, Gunma, Japan). Briefly, patellar tendons of WT mice and $OPN^{-/-}$ mice were plated in the medium and cultured for 20 days. Culture supernatants of 2nd passage fibroblasts (1×10^4 cells/ml) were collected and subjected to an ELISA analysis. Absorbance at 450 nm was measured with a microplate reader (Bio-Rad, Richmond, CA).

4.6. Quantitative analyses by transmission electron microscopy (TEM)

WT mice and $OPN^{-/-}$ mice were used for this analysis. At 10, 20 and 42 days after femoral nerve transection, the patellar tendons from both knees in each mouse were removed. A 1 mm-thick specimen sliced perpendicular to the longitudinal axis of the patellar tendon axis was cut from each block, and fixed in glutaraldehyde and osmium tetroxide. The specimen was dehydrated and embedded in epoxy resin. Ultrathin sections, approximately 80 nm, were cut perpendicular to the longitudinal axis of each specimen. The sections were stained with uranyl acetate and lead citrate for transmission electron microscopy (JEM-100CX, Nihon Denshi, Tokyo, Japan). For quantitative analyses, a randomly selected electron micrograph was taken at a final magnification of ×30,000. The diameters of all collagen fibrils in a 4 μm^2 area chosen from each micrograph were measured using an image analysis software (Win Roof; Mitani Corporation, Tokyo, Japan). A histogram of the diameters of the collagen fibrils for each patellar tendon was obtained from summation of the results of the analysis. For each group, an average histogram was made by calculating the histogram data obtained. The ratio of the total cross-sectional area of collagen fibrils to the whole visualized area was defined as the fibril occupation ratio, and this value was calculated for each patellar tendon. The fibril occupation ratio, and the number of collagen fibrils in a 1 μm^2 were also measured using image analysis software.

4.7. Purification of OPN protein

Chinese hamster ovary (CHO) cells stably transfected with murine OPN cDNA were established. Culture supernatant of transfectants was applied to a formyl-cellulofine column

(Seikagaku Kogyo, Tokyo, Japan) coupled with purified IgG from rabbit immunized with synthetic peptide, KSRSFQVSDE QYPDATDE (referred to as M3 antibody). Eluted fraction with 0.2 M glycine-HCl, pH 2.5 was immediately neutralized and dialyzed against PBS and was referred to as mOPN/CHO. OPN concentration was quantified with OPN ELISA kit (IBL, Gunma, Japan).

4.8. Cell culture of fibroblasts

Fibroblasts were isolated from the patellar tendons of B6 male WT mice and $OPN^{-/-}$ mice at various time points after surgery as described previously (Nagineni et al., 1992). The culture medium used in the present study was made from TIL medium (IBL, Gunma, Japan) supplemented with 10% fetal calf serum. The cells (2×10^4 cells/ml) were serum-starved and GRGDS peptide (100 μg/ml, ASAHI TECHNO GLASS Co., Tokyo, Japan), GRGES peptide (100 μg/ml, ASAHI TECHNO GLASS Co., Tokyo, Japan), anti-αv integrin antibody (Ab) (RMV7) (50 μg/ml, PharMingen, San Diego, CA), control anti-rat IgG (50 μg/ml, West Grove, PA), M5 Ab (30 μg/ml), M3 Ab (30 μg/ml), or mOPN/CHO protein (10 μg/ml) was added and incubated for 48 h. Total RNA from cells was extracted and MMP-13 mRNA expression was measured by real-time PCR.

4.9. Anti-OPN antibodies

The M5 Ab was generated by immunizing rabbit with a synthetic peptide, VDVPNGRGDSLAYGLRS, corresponding to the internal sequence of mouse OPN and could inhibit the interaction of OPN with its receptors as described previously (Yamamoto et al., 2003). The M3 Ab does not interfere with the binding of OPN to its receptors.

4.10. Statistical analysis

All data were represented as mean±SE. Significant differences between two groups were determined with using an unpaired Student's *t*-test. The significance level was set at 0.05. $*P<0.05$ *versus* control; $**P<0.001$ *versus* control; NS, not significantly different.

Acknowledgements

The authors acknowledge the support of grant-in-aid for scientific research from the Ministry of Education, Culture, Sports, Science and Technology (17659457), grant-in-aid from the New Energy and Industrial Technology Development Organization (03A04002a), and grant-in aid from the Nakatomi Foundation Tokyo, Japan.

References

Agnihotri, R., Crawford, H.C., Haro, H., Matrisian, L.M., Havrda, M.C., Liaw, L., 2001. Osteopontin, a novel substrate for matrix metalloproteinase-3 (stromelysin-1) and matrix metalloproteinase-7 (matrilysin). J. Biol. Chem. 276, 28261–28267.

Arnoczky, S.P., Tian, T., Lavagnino, M., Gardner, K., 2004. Ex vivo static tensile based mechanotransduction mechanism. J. Orthop. Res. 22, 328–333.

Asou, Y., Rittling, S.R., Yoshitake, H., Tsuji, K., Shinomiya, K., Nifuji, A., Denhardt, D.T., Noda, M., 2001. Osteopontin facilitates angiogenesis, accumulation of osteoclasts, and resorption in ectopic bone. Endocrinology 142, 1325–1332.

Balbin, M., Fueyo, A., Knauper, V., Pendas, A.M., Lopez, J.M., Jimenez, M.G., Murphy, G., Lopez-Otin, C., 1998. Collagenase 2 (MMP-8) expression in murine tissue-remodeling processes. Analysis of its potential role in postpartum involution of the uterus. J. Biol. Chem. 273, 23959–23968.

Balbin, M., Fueyo, A., Knauper, V., Lopez, J.M., Alvarez, J., Sanchez, L.M., Quesada, V., Bordallo, J., Murphy, G., Lopez-Otin, C., 2001. Identification and enzymatic characterization of two diverging murine counterparts of human interstitial collagenase (MMP-1) expressed at sites of embryo implantation. J. Biol. Chem. 276, 10253–10262.

Carron, C.P., Meyer, D.M., Engleman, V.W., Rico, J.G., Ruminski, P.G., Ornberg, R.L., Westlin, W.F., Nickols, G.A., 2000. Peptidomimetic antagonists of alphavbeta3 inhibit bone resorption by inhibiting osteoclast bone resorptive activity, not osteoclast adhesion to bone. J. Endocrinol. 165, 587–598.

Chung, L., Dinakarpandian, D., Yoshida, N., Lauer-Fields, J.L., Fields, G.B., Visse, R., Nagase, H., 2004. Collagenase unwinds triple-helical collagen prior to peptide bond hydrolysis. EMBO J. 23, 3020–3030.

Cunningham, K.D., Musani, F., Hart, D.A., Shrive, N.G., Frank, C.B., 1999. Collagenase degradation decreases collagen fibril diameters—an in vitro study of the rabbit medial collateral ligament. Connect. Tissue Res. 40, 67–74.

D'Alonzo, R.C., Kowalski, A.J., Denhardt, D.T., Nickols, G.A., Partridge, N.C., 2002. Regulation of collagenase-3 and osteocalcin gene expression by collagen and osteopontin in differentiating MC3T3-E1 cells. J. Biol. Chem. 277, 24788–24798.

Denhardt, D.T., Burger, E.H., Kazanecki, C., Krishna, S., Semeins, C.M., Klein-Nulend, J., 2001a. Osteopontin-deficient bone cells are defective in their ability to produce NO in response to pulsatile fluid flow. Biochem. Biophys. Res. Commun. 288, 448–453.

Denhardt, D.T., Giachelli, C.M., Rittling, S.R., 2001b. Role of osteopontin in cellular signaling and toxicant injury. Annu. Rev. Pharmacol. Toxicol. 41, 723–749.

Diao, H., Kon, S., Iwabuchi, K., Kimura, C., Morimoto, J., Ito, D., Segawa, T., Maeda, M., Hamuro, J., Nakayama, T., et al., 2004. Osteopontin as a mediator of NKT cell function in T cell-mediated liver diseases. Immunity 21, 539–550.

Fisher, L.W., Jain, A., Tayback, M., Fedarko, N.S., 2004. Small integrin binding ligand N-linked glycoprotein gene family expression in different cancers. Clin. Cancer Res. 10, 8501–8511.

Franzen, A., Heinegard, D., 1985. Isolation and characterization of two sialoproteins present only in bone calcified matrix. Biochem. J. 232, 715–724.

Hasty, K.A., Pourmotabbed, T.F., Goldberg, G.I., Thompson, J.P., Spinella, D.G., Stevens, R.M., Mainardi, C.L., 1990. Human neutrophil collagenase. A distinct gene product with homology to other matrix metalloproteinases. J. Biol. Chem. 265, 11421–11424.

Henriet, P., Rousseau, G.G., Eeckhout, Y., 1992. Cloning and sequencing of mouse collagenase cDNA. Divergence of mouse and rat collagenases from the other mammalian collagenases. FEBS Lett. 310, 175–178.

Hirata, A., Masuda, S., Tamura, T., Kai, K., Ojima, K., Fukase, A., Motoyoshi, K., Kamakura, K., Miyagoe-Suzuki, Y., Takeda, S., 2003. Expression profiling of cytokines and related genes in regenerating skeletal muscle after cardiotoxin injection: a role for osteopontin. Am. J. Pathol. 163, 203–215.

Humphries, J.D., Schofield, N.R., Mostafavi-Pour, Z., Green, L.J., Garratt, A.N., Mould, A.P., Humphries, M.J., 2005. Dual functionality of the anti-beta1 integrin antibody, 12G10, exemplifies agonistic signalling from the ligand binding pocket of integrin adhesion receptors. J. Biol. Chem. 280, 10234–10243.

Ishijima, M., Rittling, S.R., Yamashita, T., Tsuji, K., Kurosawa, H., Nifuji, A., Denhardt, D.T., Noda, M., 2001. Enhancement of osteoclastic bone

resorption and suppression of osteoblastic bone formation in response to reduced mechanical stress do not occur in the absence of osteopontin. J. Exp. Med. 193, 399–404.

Jain, A., Brennan, F., Troeberg, L., Nanchahal, J., 2002. The role of matrix metalloproteinases in rheumatoid tendon disease. J. Hand Surg. [Am.] 27, 1059–1064.

Kannus, P., Jozsa, L., Renstrom, P., Jarvinen, M., Kvist, M., Lehto, M., Oja, P., Vuori, I., 1992. The effects of training, immobilization and remobilization on musculoskeletal tissue. Training and immobilization. Scand. J. Med. Sci. Sports 2, 100–118.

Kannus, P., Jozsa, L., Natri, A., Jarvinen, M., 1997. Effects of training, immobilization and remobilization on tendons. Scand. J. Med. Sci. Sports 7, 67–71.

Katagiri, Y.U., Sleeman, J., Fujii, H., Herrlich, P., Hotta, H., Tanaka, K., Chikuma, S., Yagita, H., Okumura, K., Murakami, M., Saiki, I., Chambers, A., Uede, T., 1999. CD44 variants but not CD44s cooperate with beta1-containing integrins to permit cells to bind to osteopontin independently of arginine–glycine–aspartic acid, thereby stimulating cell motility and chemotaxis. Cancer Res. 59, 219–226.

Khan, S.A., Lopez-Chua, C.A., Zhang, J., Fisher, L.W., Sorensen, E.S., Denhardt, D.T., 2002. Soluble osteopontin inhibits apoptosis of adherent endothelial cells deprived of growth factors. J. Cell. Biochem. 85, 728–736.

Kon, S., Maeda, M., Segawa, T., Hagiwara, Y., Horikoshi, Y., Chikuma, S., Tanaka, K., Rashid, M.M., Inobe, M., Chambers, A.F., Uede, T., 2000. Antibodies to different peptides in osteopontin reveal complexities in the various secreted forms. J. Cell. Biochem. 77, 487–498.

Lavagnino, M., Arnoczky, S.P., Frank, K., Tian, T., 2005. Collagen fibril diameter distribution does not reflect changes in the mechanical properties of in vitro stress-deprived tendons. J. Biomech. 38, 69–75.

Liaw, L., Skinner, M.P., Raines, E.W., Ross, R., Cheresh, D.A., Schwartz, S.M., Giachelli, C.M., 1995. The adhesive and migratory effects of osteopontin are mediated via distinct cell surface integrins. Role of alpha v beta 3 in smooth muscle cell migration to osteopontin in vitro. J. Clin. Invest. 95, 713–724.

Liaw, L., Birk, D.E., Ballas, C.B., Whitsitt, J.S., Davidson, J.M., Hogan, B.L., 1998. Altered wound healing in mice lacking a functional osteopontin gene (spp1). J. Clin. Invest. 101, 1468–1478.

Majima, T., Yasuda, K., Fujii, T., Yamamoto, N., Hayashi, K., Kaneda, K., 1996. Biomechanical effects of stress shielding of the rabbit patellar tendon depend on the degree of stress reduction. J. Orthop. Res. 14, 377–383.

Majima, T., Marchuk, L.L., Shrive, N.G., Frank, C.B., Hart, D.A., 2000. In-vitro cyclic tensile loading of an immobilized and mobilized ligament autograft selectively inhibits mRNA levels for collagenase (MMP-1). J. Orthop. Sci. 5, 503–510.

Majima, T., Yasuda, K., Tsuchida, T., Tanaka, K., Miyakawa, K., Minami, A., Hayashi, K., 2003. Stress shielding of patellar tendon: effect on small-diameter collagen fibrils in a rabbit model. J. Orthop. Sci. 8, 836–841.

Meazzini, M.C., Toma, C.D., Schaffer, J.L., Gray, M.L., Gerstenfeld, L.C., 1998. Osteoblast cytoskeletal modulation in response to mechanical strain in vitro. J. Orthop. Res. 16, 170–180.

Nagineni, C.N., Amiel, D., Green, M.H., Berchuck, M., Akeson, W.H., 1992. Characterization of the intrinsic properties of the anterior cruciate and medial collateral ligament cells: an in vitro cell culture study. J. Orthop. Res. 10, 465–475.

Nomura, S., Takano-Yamamoto, T., 2000. Molecular events caused by mechanical stress in bone. Matrix Biol. 19, 91–96.

Ogbureke, K.U., Fisher, L.W., 2004. Expression of SIBLINGs and their partner MMPs in salivary glands. J. Dent. Res. 83, 664–670.

O'Regan, A., Berman, J.S., 2000. Osteopontin: a key cytokine in cell-mediated and granulomatous inflammation. Int. J. Exp. Pathol. 81, 373–390.

Philip, S., Bulbule, A., Kundu, G.C., 2001. Osteopontin stimulates tumor growth and activation of promatrix metalloproteinase-2 through nuclear factor-kappa B-mediated induction of membrane type 1 matrix metalloproteinase in murine melanoma cells. J. Biol. Chem. 276, 44926–44935.

Rangaswami, H., Bulbule, A., Kundu, G.C., 2004. Nuclear factor-inducing kinase plays a crucial role in osteopontin-induced MAPK/IkappaBalpha kinase-dependent nuclear factor kappaB-mediated promatrix metalloproteinase-9 activation. J. Biol. Chem. 279, 38921–38935.

Rittling, S.R., Matsumoto, H.N., McKee, M.D., Nanci, A., An, X.R., Novick, K.E., Kowalski, A.J., Noda, M., Denhardt, D.T., 1998. Mice lacking osteopontin show normal development and bone structure but display altered osteoclast formation in vitro. J. Bone Miner. Res. 13, 1101–1111.

Ronziere, M.C., Aubert-Foucher, E., Gouttenoire, J., Bernaud, J., Herbage, D., Mallein-Gerin, F., 2005. Integrin alpha1beta1 mediates collagen induction of MMP-13 expression in MC615 chondrocytes. Biochim. Biophys. Acta 1746, 55–64.

Salingcarnboriboon, R., Yoshitake, H., Tsuji, K., Obinata, M., Amagasa, T., Nifuji, A., Noda, M., 2003. Establishment of tendon-derived cell lines exhibiting pluripotent mesenchymal stem cell-like property. Exp. Cell Res. 287, 289–300.

Sharma, P., Maffulli, N., 2005. Tendon injury and tendinopathy: healing and repair. J. Bone Jt. Surg., Am. 87, 187–202.

Singh, R.P., Patarca, R., Schwartz, J., Singh, P., Cantor, H., 1990. Definition of a specific interaction between the early T lymphocyte activation 1 (Eta-1) protein and murine macrophages in vitro and its effect upon macrophages in vivo. J. Exp. Med. 171, 1931–1942.

Sodek, J., Ganss, B., McKee, M.D., 2000. Osteopontin. Crit. Rev. Oral Biol. Med. 11, 279–303.

Terai, K., Takano-Yamamoto, T., Ohba, Y., Hiura, K., Sugimoto, M., Sato, M., Kawahata, H., Inaguma, N., Kitamura, Y., Nomura, S., 1999. Role of osteopontin in bone remodeling caused by mechanical stress. J. Bone Miner. Res. 14, 839–849.

Trueblood, N.A., Xie, Z., Communal, C., Sam, F., Ngoy, S., Liaw, L., Jenkins, A.W., Wang, J., Sawyer, D.B., Bing, O.H., et al., 2001. Exaggerated left ventricular dilation and reduced collagen deposition after myocardial infarction in mice lacking osteopontin. Circ. Res. 88, 1080–1087.

Uede, T., Katagiri, Y., Iizuka, J., Murakami, M., 1997. Osteopontin, a coordinator of host defense system: a cytokine or an extracellular adhesive protein? Microbiol. Immunol. 41, 641–648.

Vincenti, M.P., Coon, C.I., Mengshol, J.A., Yocum, S., Mitchell, P., Brinckerhoff, C.E., 1998. Cloning of the gene for interstitial collagenase-3 (matrix metalloproteinase-13) from rabbit synovial fibroblasts: differential expression with collagenase-1 (matrix metalloproteinase-1). Biochem. J. 331 (Pt 1), 341–346.

Weber, G.F., Askar, S., Glimcher, M.J., Cantor, H., 1996. Receptor–ligand interaction between CD44 and osteopontin (Eta-1). Science 271, 509–512.

Weintraub, A.S., Schnapp, L.M., Lin, X., Taubman, M.B., 2000. Osteopontin deficiency in rat vascular smooth muscle cells is associated with an inability to adhere to collagen and increased apoptosis. Lab. Invest. 80, 1603–1615.

Xie, Z., Singh, M., Siwik, D.A., Joyner, W.L., Singh, K., 2003. Osteopontin inhibits interleukin-1beta-stimulated increases in matrix metalloproteinase activity in adult rat cardiac fibroblasts: role of protein kinase C-zeta. J. Biol. Chem. 278, 48546–48552.

Yamamoto, N., Sakai, F., Kon, S., Morimoto, J., Kimura, C., Yamazaki, H., Okazaki, I., Seki, N., Fujii, T., Uede, T., 2003. Essential role of the cryptic epitope SLAYGLR within osteopontin in a murine model of rheumatoid arthritis. J. Clin. Invest. 112, 181–188.

Zhang, D., Liu, M., Ding, F., Gu, X., 2006. Expression of myostatin RNA transcript and protein in gastrocnemius muscle of rats after sciatic nerve resection. J. Muscle Res. Cell Motil. 1–8.

Zohar, R., Zhu, B., Liu, P., Sodek, J., McCulloch, C.A., 2004. Increased cell death in osteopontin-deficient cardiac fibroblasts occurs by a caspase-3-independent pathway. Am. J. Physiol, Heart Circ. Physiol. 287, H1730–H1739.

ARTHRITIS & RHEUMATISM
Vol. 56, No. 2, February 2007, pp 521–530
DOI 10.1002/art.22407

A Novel DNA Vaccine Targeting Macrophage Migration Inhibitory Factor Protects Joints From Inflammation and Destruction in Murine Models of Arthritis

Shin Onodera,[1] Shigeki Ohshima,[1] Harukazu Tohyama,[1] Kazunori Yasuda,[1] Jun Nishihira,[2] Yoichiro Iwakura,[3] Ikkei Matsuda,[4] Akio Minami,[1] and Yoshikazu Koyama[1]

Objective. **Previous studies have demonstrated that neutralization of macrophage migration inhibitory factor (MIF) by anti-MIF antibodies decreases joint inflammation and destruction in a type II collagen–induced arthritis model in mice. The aim of this study was to develop and describe a simple and effective method of active immunization that induces anti-MIF autoantibodies, which may neutralize MIF bioactivity.**

Methods. **We developed a MIF DNA vaccine by introducing oligonucleotides encoding a tetanus toxoid (TTX) Th cell epitope into the complementary DNA sequence of murine MIF. Mice were injected with this construct in conjunction with electroporation. The ability of this immunization to inhibit the development of collagen antibody–induced arthritis (CAIA) in BALB/c mice and spontaneous autoimmune arthritis in interleukin-1 receptor antagonist (IL-1Ra)–deficient mice was then evaluated.**

Results. **Mice that received the MIF/TTX DNA vaccine developed high titers of autoantibodies that reacted to native MIF. Compared with unvaccinated mice, vaccinated mice also produced less serum tumor necrosis factor α after receiving an intravenous injection of lipopolysaccharide. In addition, vaccination with MIF/TTX DNA resulted in significant amelioration of both CAIA in BALB/c mice and symptoms of autoimmune arthritis in IL-1Ra–knockout mice.**

Conclusion. **These results suggest that MIF/TTX DNA vaccination may be useful for ameliorating the symptoms of rheumatoid arthritis.**

Recent reevaluation of macrophage migration inhibitory factor (MIF) has suggested that MIF may be an important mediator of various inflammatory diseases. In particular, increasing evidence suggests that MIF plays a key role in the pathogenesis of rheumatoid arthritis (RA) (1). For example, we previously reported that in the rheumatoid synovium, MIF is expressed exclusively in synovial T cells, and that MIF levels in joint fluid are much higher in patients with RA than in patients with osteoarthritis (OA) or normal volunteers (2). Moreover, MIF is known to induce macrophages to produce tumor necrosis factor α (TNFα) and nitric oxide (3) and has been shown to up-regulate matrix metalloproteinases and cyclooxygenase 2 messenger RNA in rheumatoid synovial fibroblasts (4,5). Furthermore, MIF-deficient mice are protected from antigen-induced arthritis and arthritis induced by anti–type II collagen antibodies (collagen antibody–induced arthritis [CAIA]) (6,7). In addition, both the synovial expression of MIF and polymorphisms in the MIF gene promoter have been reported to correlate positively with disease activity in RA (8,9). These observations strongly suggest that MIF plays an important role in the pathomechanism of RA.

Monoclonal antibodies to MIF have been shown to inhibit joint inflammation profoundly in rodent models of RA (10,11). However, the therapeutic utility of such monoclonal antibodies is limited by 1) the massive

Supported in part by grants-in-aid from the Ministry of Science and Education (no. 15591560), the Hip Joint Foundation of Japan, and the Uehara Memorial Foundation.

[1]Shin Onodera, MD, Shigeki Ohshima, MD, Harukazu Tohyama, MD, Kazunori Yasuda, MD, Akio Minami, MD, Yoshikazu Koyama, PhD: Hokkaido University Graduate School of Medicine, Sapporo, Japan; [2]Jun Nishihira, MD: GeneticLab Co., Sapporo, Japan; [3]Yoichiro Iwakura, MD: Center for Experimental Medicine, Institute of Medical Science, University of Tokyo, Tokyo, Japan; [4]Ikkei Matsuda: Institute for Genetic Medicine, Hokkaido University, Sapporo, Japan.

Address correspondence and reprint requests to Yoshikazu Koyama, PhD, Department of Biochemistry, Hokkaido University Graduate School of Medicine, Sapporo 060-8638, Japan. E-mail: y_koyama@med.hokudai.ac.jp.

Submitted for publication June 30, 2006; accepted in revised form November 9, 2006.

amounts of antibody that must be injected each time (which could generate transient undesirable local and systemic reactions); 2) the short duration of the protective effects because of a lack of immune B cell memory, which necessitates frequent injections; and 3) the fact that either humanized antibodies (which are usually of low affinity) or heterogeneous antibodies (the repeated administration of which will probably generate an anti-antibody response) would have to be used (12). To overcome these limitations, researchers have sought to develop therapeutic vaccines that will elicit autoantibodies against target proteins such as cytokines or pathogens.

The aim of the current study was to develop a vaccine that would generate endogenous anti-MIF antibodies. This was achieved by constructing the MIF/tetanus toxoid (TTX) DNA vaccine, which encodes a variant of murine MIF (mMIF), the second loop of which is replaced by a promiscuous Th cell epitope from tetanus toxin. The ability of this vaccine to inhibit the development of arthritis was tested in 2 different murine arthritis models. One of these models is CAIA, which is induced in BALB/c mice by injection with a cocktail of anti–type II collagen monoclonal antibodies followed by an injection of lipopolysaccharide (LPS). This is a self-limiting arthritis, the symptoms of which last for ~3–4 weeks after administration of the monoclonal antibodies. The other model involves interleukin-1 receptor antagonist (IL-Ra)–deficient mice, which at ~5 weeks of age spontaneously develop an autoimmune polyarthritis that is characterized by enhanced levels of serum autoantibodies against immunoglobulin, type II collagen, and double-stranded DNA. In close to 100% of the mice in both models, arthritis develops in the limb joints.

MATERIALS AND METHODS

Mice. BALB/c mice (4 weeks old) were purchased from Sankyou Laboratory Service (Shizuoka, Japan) and were maintained under specific pathogen–free conditions. IL-1Ra–knockout mice were generated as previously described (13). All animal procedures were conducted according to the guidelines of the Hokkaido University Institutional Animal Care and Use Committee under an approved protocol. Female adult mice (4 weeks of age) were used in each experiment.

Construction of the MIF/TTX expression plasmid. Murine MIF complementary DNA (cDNA) was cloned into the mammalian expression vector pCAGGS (14). To generate an immunologically active MIF antigen, an MIF variant whose second loop region is replaced by a TTX Th cell epitope was designed. For this purpose, the cDNA region that encodes the second loop of mMIF (amino acids 32–37 [GKPAQY]) was deleted from the MIF cDNA and substituted with an *Eco* RI site by standard polymerase chain reaction–based techniques. Complementary DNA encoding the TTX p30 Th cell epitope (FNNFTVSFWLRVPKVSASHL) (15) with an *Eco* RI site at both termini was obtained by hybridization of partially overlapping oligo DNAs (sense, GAATTCAACAACTTCACCGTGAGCTTCTGGCTGCGCGTGCCCAA; anti-sense, GGAATTCCAGGTGGCTGGCGCTCACCTTGGGCACGCGCAGCCAGA) and subsequent polymerization with the *Klenow* fragment of DNA polymerase. After digestion with *Eco* RI, the p30 cDNA was inserted into the *Eco* RI site of the MIF expression plasmid (Figure 1), and a clone bearing a correctly oriented insert was selected. The MIF/TTX plasmid DNA was then purified by alkaline lysis followed by 2 rounds of CsCl density-gradient ultracentrifugation. This preparation was used for animal vaccination.

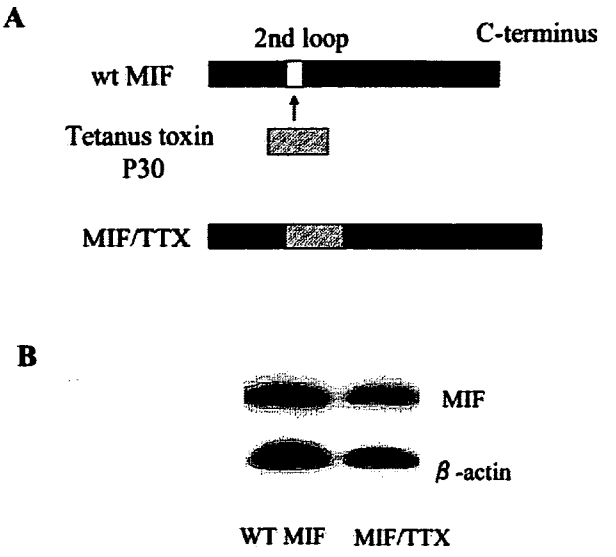

Figure 1. Design and antigenicity of the macrophage migration inhibitory factor (MIF)/tetanus toxoid (TTX) DNA vaccine. **A,** Design of a DNA construct that expresses a murine MIF (mMIF) variant, the second loop of which bears a promiscuous Th cell epitope from TTX. To generate this construct, mMIF cDNA was cloned into the mammalian expression vector pCAGGS, after which the second loop region of MIF cDNA was substituted with the Th cell epitope. **B,** Expression and antigenicity of wild-type (WT) MIF and MIF/TTX DNAs. COS-7 cells were transiently transfected with the DNA constructs expressing either WT MIF or MIF/TTX, and their lysates were analyzed by Western blotting using rabbit anti-mMIF antibody. Results are representative of 3 independent experiments.

Analysis of in vitro expression of MIF/TTX. COS-7 cells were transfected with either the expression plasmid for wild-type (WT) MIF or MIF/TTX by using Effectene transfection reagent (Qiagen, Valencia, CA) according to the method recommended by the manufacturer. After 24 hours, the cells were lysed with 1% Nonidet P40/20 m*M* Tris HCl, pH 7.6/20% glycerol/1 m*M* EDTA/1 m*M* phenylmethylsulfonyl fluoride. The extracts were then subjected to sodium dodecyl sulfate–polyacrylamide gel electrophoresis and blotted onto

polyvinylidene difluoride membranes, which were subsequently blocked with 3% skim milk and then incubated with rabbit anti-MIF antibody. After reacting the membranes with horseradish peroxidase (HRP)–conjugated donkey anti-rabbit antibody, the MIF protein was visualized by using a chemiluminescence system (Amersham, Arlington Heights, IL).

Intramuscular DNA injection and electroporation. Gene transfer into muscle by electroporation was performed essentially as described previously (16). Mice were anesthetized with ether and shaved around their hind legs, after which a pair of electrode needles (5-mm gap and 0.5-mm diameter; Nepa Gene, Chiba, Japan) were inserted into an anterior tibial muscle, and the DNA vaccine (25 μg/25 μl 0.9% saline) was injected into the portion between the needles. Three electric pulses (50V and 50 msec) were applied by using an electric pulse generation system (T820 and Optimizer 500; BTX, San Diego, CA) and were followed by another 3 pulses with inverted polarity. The other tibial muscle was then also injected and subjected to electroporation. As a result, each mouse received 50 μg of the naked plasmid. A similar vaccination procedure was repeated 3 weeks later.

Evaluation of anti-MIF antibody titers in sera from DNA-vaccinated mice. Anti-MIF titers in plasma were determined by direct enzyme-linked immunosorbent assay (ELISA). Briefly, individual plasma samples from vaccinated mice were collected from the tail vein and diluted with 0.1% bovine serum albumin/phosphate buffered saline (PBS)/0.05% Tween 20. Small aliquots of diluted plasma (1:200) were added to 96-well flat-bottomed plates precoated with recombinant mMIF. The serum anti-MIF antibodies that reacted with the precoated MIF were detected by HRP-conjugated goat anti-mouse antibody, followed by color development with a substrate reagent (Techne, Minneapolis, MN). Antibodies raised in the vaccinated animals were also tested for their ability to compete with a specific mouse monoclonal antibody for MIF antigen. Thus, microtiter plates were precoated with the anti-MIF monoclonal antibody XIV.14.3 (a kind gift from Dr. Richard Bucala, Yale University). The pooled plasma samples from animals that had been vaccinated with the MIF/TTX vaccine or the control pCAGGS plasmid were serially diluted and preincubated with recombinant mMIF. The reaction mixtures were then added to the microtiter plate, incubated for 1 hour, and washed. The amount of MIF bound by the XIV.14.3 monoclonal antibody was then determined by serial incubation, first with biotin-labeled rabbit anti-MIF antibody and then with HRP-conjugated biotin–streptavidin complex (Amersham).

Measurement of serum TNFα. It has been reported that, compared with untreated mice, mice treated with a polyclonal anti-MIF antibody produce less serum TNFα after intravenous injection with LPS (17). We tested whether the anti-MIF antibodies raised by MIF/TTX DNA vaccination have the same suppressive activity. Thus, 6 weeks after administering the MIF/TTX vaccine or the control pCAGGS construct once to 4-week-old BALB/c mice, each mouse was injected intravenously with 200 μl of a mixture of LPS (0111:B4; 1μg/ml) and D-galactosamine (60 mg/ml). Blood samples (5 μl) were then collected from the tail vein every 1.5 hours, and serum concentrations of TNFα were measured by using a mouse TNFα ELISA kit (BioSource, Camarillo, CA) according to the manufacturer's protocol.

Initiation of CIA and evaluation of arthritis. Arthritis antibody kits were obtained from Immuno-Biological Laboratories (Gumma, Japan), and arthritis was induced according to the manufacturer's instructions (18). Briefly, 2 weeks after receiving their second DNA immunization, BALB/c mice were injected intraperitoneally with a mixture of 4 anti–type II collagen monoclonal antibodies (2 mg each), followed by intraperitoneal injection with 50 μg of LPS (0111:B4) 3 days later (day 0). The incidence of arthritis was judged macroscopically by examining each joint for swelling and redness on days 1, 3, 7, 14, and 21, as described previously (19), and each joint was graded as follows: grade 0 = normal, grade 1 = light swelling of the joint and/or redness of the footpad, grade 2 = obvious swelling of the joint, and grade 3 = severe swelling and fixation of the joint. The arthritis score was calculated for all 4 limbs; thus, the maximum possible score for each mouse was 12 points.

Evaluation of arthritis in IL-1Ra–knockout mice. IL-1Ra–knockout mice were vaccinated once with MIF/TTX (n = 16) at the age of 4 weeks. Control mice were injected once with the pCAGGS vector (n = 5) or endotoxin-free saline (n = 6). The anti-mMIF titers in sera were assessed every 2 weeks, as previously described. The clinical parameters assessed were the percentage of arthritic mice, the arthritis score, and paw swelling. The arthritis score was evaluated as described above. Paw swelling was assessed by measuring the thickness of the affected hind paws with 0–10-mm calipers (Mitutoyo, Kanagawa, Japan).

Histopathology. BALB/c mice given anti–type II collagen monoclonal antibodies were killed under anesthesia on day 14, while IL-1Ra–knockout mice were killed 16 weeks after being given the DNA vaccine. The whole hind limbs of the mice were harvested, fixed in 4% paraformaldehyde in PBS, decalcified in EDTA, and then embedded in paraffin. Serial sagittal sections were subjected to hematoxylin and eosin staining for histologic analyses. For IL-1Ra–knockout mice, Safranin O and fast green/iron hematoxylin staining was added to estimate the loss of cartilage proteoglycan. Moreover, MIF protein expression was examined by immunohistochemistry using an anti-MIF antibody, as described previously (6).

Statistical analysis. For statistical analysis, one-way factorial analysis of variance was performed, followed by Fisher's protected least significant difference as a post hoc test.

RESULTS

Design of the MIF/TTX vaccine and analysis of its in vitro expression. We constructed a DNA vaccine that encoded an mMIF variant whose second loop region was replaced with a promiscuous foreign Th cell epitope from TTX (FNNFTVSFWLRVPKVSASHL) (Figure 1A). The second loop region of MIF (aa ^{32}Gly–^{37}Tyr) was selected for TTX epitope insertion on the basis of the 3-dimensional structure of MIF (20); replacement of this region rather than the other loops seemed less likely to interfere with the quaternary structure and antigenicity of the trimeric MIF complex. The chimeric MIF/TTX cDNA construct was then

cloned into the expression plasmid pCAGGS. Prior to in vivo administration, we tested whether this construct produced the right protein by transiently transfecting COS-7 cells. As shown in Figure 1B, the chimeric MIF/TTX protein showed mobility on a sodium dodecyl sulfate electrophoresis gel similar to that of WT MIF. Moreover, it was recognized by a rabbit antibody raised against WT mMIF. Thus, insertion of the foreign Th cell epitope did not affect expression of the molecule or the antigenicity of its MIF domain.

Generation of anti-MIF antibodies and production of serum TNFα in MIF/TTX-vaccinated BALB/c mice upon injection with LPS. We tested whether the DNA vaccine could induce a polyclonal antibody response that recognized native MIF. Thus, both tibial muscles of BALB/c mice were vaccinated intramuscularly with 50 μg of WT MIF, MIF/TTX, or vector DNA in 0.9% saline, with the aid of electroporation. The animals were vaccinated twice, 3 weeks apart. As shown in Figure 2A, by 4 weeks after the first vaccination, the MIF/TTX-vaccinated mice had autoantibodies that reacted to native MIF. In contrast, neither the WT MIF vaccine nor the vector vaccine raised such MIF-reactive antibodies until 12 weeks after the first vaccination. These differences were statistically significant ($P < 0.05$, MIF/TTX versus pCAGGS) and indicate that by incorporating the TTX Th cell epitope, the immunologic tolerance of mice to the MIF self protein is bypassed.

We also tested whether the anti-MIF antibodies generated by the MIF/TTX DNA vaccine could compete with a MIF-specific monoclonal antibody for the binding of native mMIF protein. A competition ELISA revealed that when the polyclonal serum antibodies from vaccinated mice were preincubated with recombinant mMIF, they could compete with anti-MIF monoclonal antibody 14.3 for binding to the MIF protein (Figure 2B).

It has been shown previously that pretreatment of mice with a polyclonal anti-MIF antibody effectively suppresses the rise in serum TNFα levels that is induced by a subsequent intravenous injection of LPS (17). Thus, we tested whether the MIF/TTX vaccine–induced anti-MIF antibodies would also have the same effect. We observed that when mice vaccinated once with MIF/TTX were injected with LPS 6 weeks after the vaccination, their serum TNFα levels were significantly lower than those of LPS-treated mice injected previously with vector DNA (Figure 2C) ($P < 0.0001$, MIF/TTX versus pCAGGS). Thus, the anti-MIF antibodies generated by the MIF/TTX DNA vaccine have antiinflammatory properties, probably because they inhibit the bioactivity of endogenous MIF.

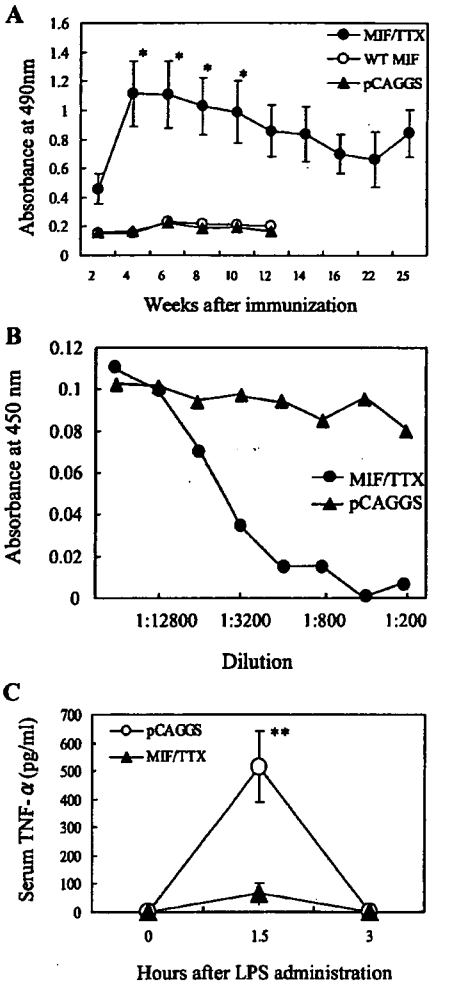

Figure 2. A, Effects of immunization with MIF/TTX DNA on elicitation of autoantibodies that recognize native mMIF. BALB/c mice were vaccinated twice, 3 weeks apart, with 50 μg of pCAGGS, WT MIF construct, or MIF/TTX construct in 0.9% endotoxin-free sterile saline (n = 5 mice per group). Serum samples from these mice were obtained at various time points, and anti-MIF antibody levels were measured by enzyme-linked immunosorbent assay (ELISA), using microtiter plates coated with recombinant mMIF. * = $P < 0.05$, MIF/TTX versus pCAGGS. B, Ability of polyclonal anti-MIF antibodies generated by MIF/TTX DNA vaccination to compete with anti-MIF monoclonal antibody 14.3 for binding to recombinant MIF. A competitive ELISA was performed by preincubating pooled sera from the pCAGGS- or MIF/TTX-vaccinated mice described in A with recombinant mMIF and then adding the mixtures to a microtiter plate on which monoclonal antibody 14.3 had been immobilized. C, Effect of MIF/TTX DNA vaccination on lipopolysaccharide (LPS)–induced rise in serum tumor necrosis factor α (TNFα) levels. Mice immunized with MIF/TTX or vector DNA were injected intravenously with LPS 6 weeks after the vaccination. Serum TNFα levels were measured by ELISA. Values are the mean ± SEM. ** = $P < 0.0001$, MIF/TTX versus pCAGGS. See Figure 1 for other definitions.

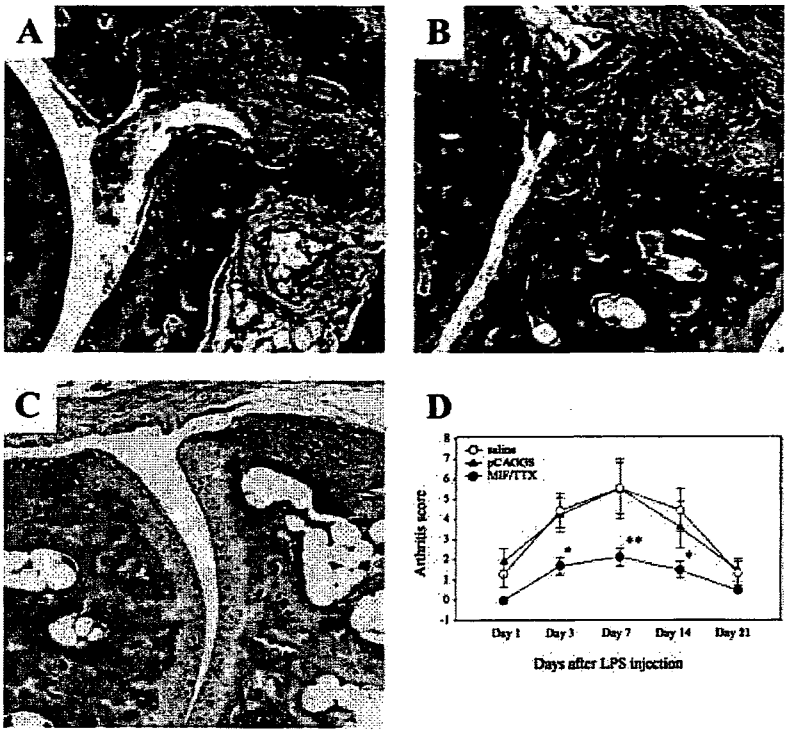

Figure 3. Representative results of histologic analysis of tarsocrural joints from **A**, saline-treated, **B**, pCAGGS-vaccinated, and **C**, MIF/TTX-vaccinated BALB/c mice on day 14. Marked changes were observed in specimens obtained from saline-treated and pCAGGS-vaccinated mice, including synovial hyperplasia, inflammatory cell infiltration, extensive pannus formation at the cartilage–bone junction, and severe cartilage destruction. Specimens obtained from some of the MIF/TTX-vaccinated mice revealed only slight thickening and proliferation of the synovial lining, mild inflammatory cell infiltration, no pannus invasion, and intact bone and cartilage structure. (Original magnification × 200.) **D**, Arthritis scores (degree of arthritis in all 4 joints of each mouse) following injection of lipopolysaccharide (LPS). Values are the mean ± SEM. * = $P < 0.05$, ** = $P < 0.005$, MIF/TTX versus pCAGGS. See Figure 1 for other definitions.

We also attempted to measure the ability of the immune sera to inhibit the in vitro production of TNFα by LPS-stimulated peritoneal macrophages. However, reproducible results could not be obtained, possibly because the sera interfered nonspecifically with TNFα production. A similar failure has been reported previously (21). Nevertheless, these observations together indicate that immunization with MIF/TTX DNA generated antibodies that can specifically recognize native mMIF and probably neutralize the bioactivity of this molecule.

Effect of vaccination with MIF/TTX DNA on the development and severity of CIA. In mice with CAIA, the endogenous production of MIF is enhanced, and antibodies to MIF have been shown to profoundly inhibit joint inflammation (7). Thus, we tested whether the MIF/TTX DNA vaccine would inhibit the development of CAIA in this murine model of rheumatoid arthritis by immunizing 16 BALB/c mice twice with MIF/TTX DNA. As controls, we also immunized 6 mice with saline and 5 mice with pCAGGS vector. For histologic evaluation, 3 groups consisting of 3–4 BALB/c mice, respectively, were prepared as described above. Two weeks after the second immunization, the mice were injected first with anti–type II collagen monoclonal antibodies and then 3 days later were injected with LPS.

Histologic analysis of the saline- or pCAGGS-treated mice on day 14 revealed marked pathologic changes in the tarsocrural joint tissues; these changes included synovial hyperplasia, inflammatory cell infiltra-

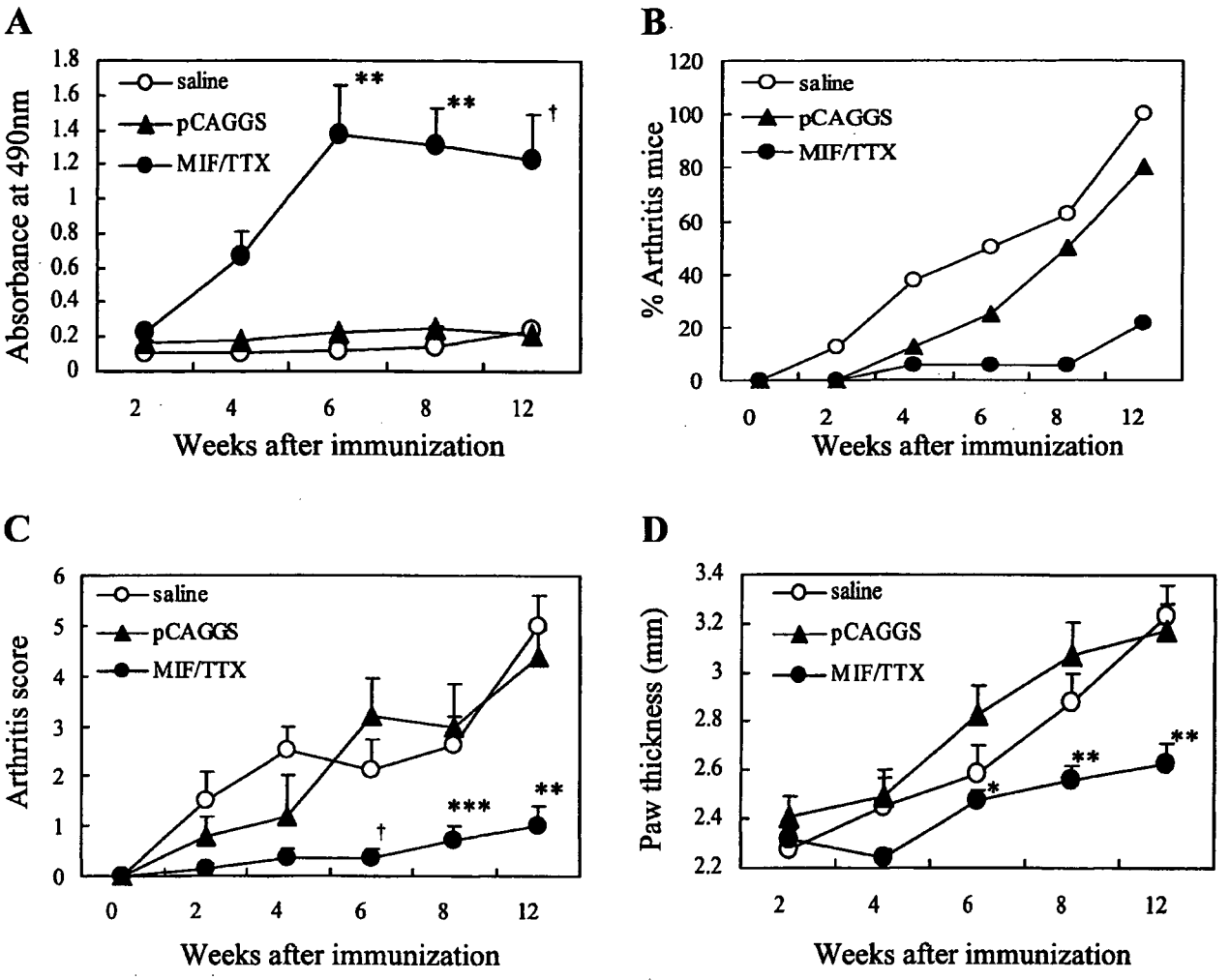

Figure 4. The MIF/TTX DNA vaccine inhibits the development of spontaneous autoimmune arthritis in interleukin-1 receptor antagonist (IL-1Ra)–knockout mice and reduces its severity. Four-week-old IL-1Ra–knockout mice were vaccinated once with MIF/TTX (n = 16), pCAGGS vector (n = 5), or endotoxin-free saline (n = 6). **A,** Anti-mMIF serum titers. **B,** Percentage of arthritic mice. **C,** Arthritis score. **D,** Degree of hind paw swelling. Values are the mean and SEM. * = $P < 0.05$; ** = $P < 0.0001$; *** = $P < 0.001$; † = $P < 0.005$, MIF/TTX versus pCAGGS. See Figure 1 for other definitions.*

tion, extensive pannus formation at the cartilage–bone junction, and severe cartilage destruction (Figures 3A and B). In contrast, histologic sections of the tarsocrural joints from some of the MIF/TTX-vaccinated mice revealed only slight thickening and proliferation of the synovial lining, mild inflammatory cell infiltration, no pannus invasion, and intact bone and cartilage structure (Figure 3C). Moreover, among animals examined on days 3, 7, and 14, the MIF/TTX-vaccinated mice had significantly lower arthritis scores compared with controls, which indicated that the severity of clinical symptoms of arthritis was reduced in these animals ($P < 0.05$ and $P < 0.005$, MIF/TTX versus pCAGGS) (Figure 3D).

Effect of vaccination with MIF/TTX DNA on the development of autoimmune arthritis in IL-1Ra–knockout mice. We also examined whether the MIF/TTX vaccine can act to block the severity of spontaneous arthritis in IL-Ra–knockout mice. Thus, we immunized IL-1Ra–knockout mice with MIF/TTX DNA, pCAGGS DNA, or saline once at age 4 weeks. Analysis of the anti-MIF antibody titers generated over time in these mice revealed significantly elevated titers 6

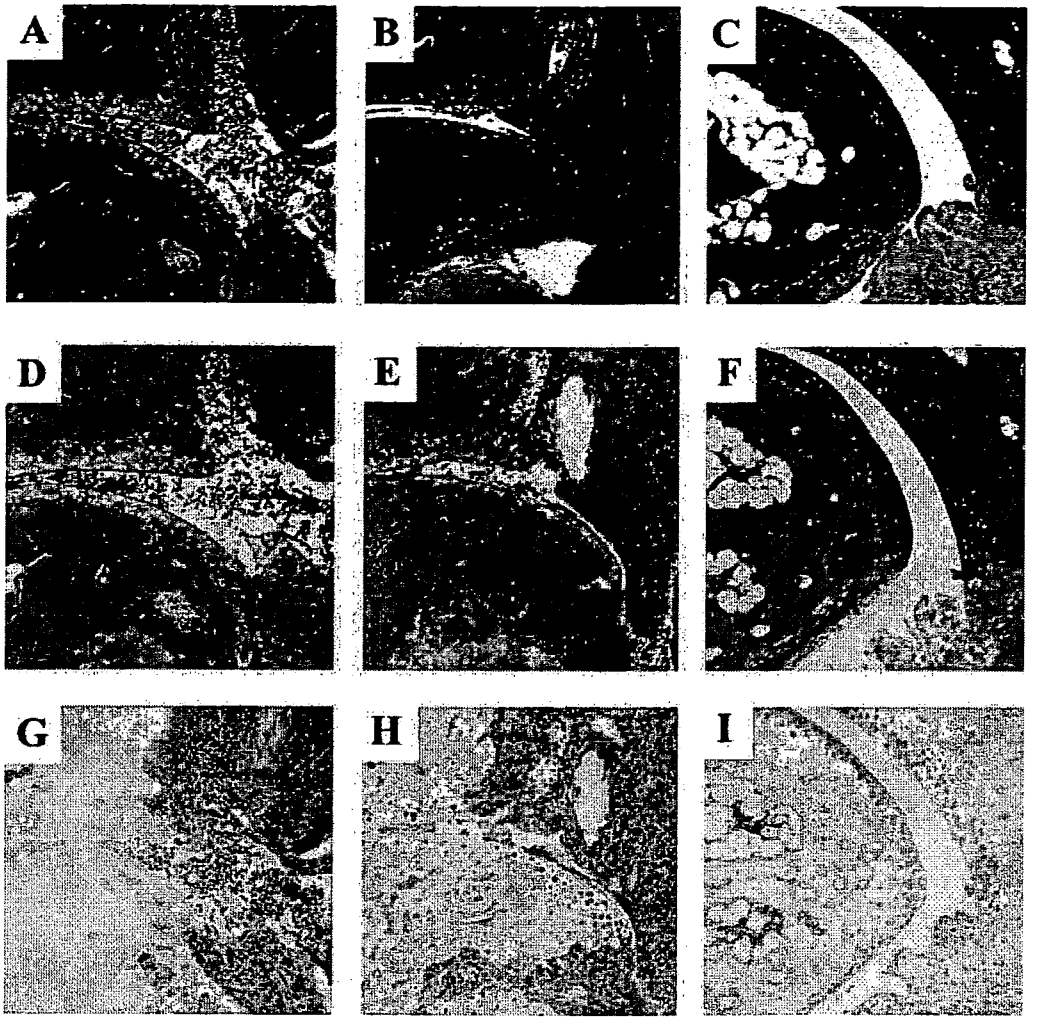

Figure 5. Representative results of histologic analysis of the effects of vaccination with saline (**A, D,** and **G**), pCAGGS (**B, E,** and **H**), or macrophage migration inhibitory factor/tetanus toxoid (**C, F,** and **I**). Ankle joints from interleukin-1 receptor antagonist (IL-1Ra)–knockout mice were collected 16 weeks after vaccination, and specimens were stained with hematoxylin and eosin (**A–C**) or Safranin O (**D–F**), or were immunohistologically stained with polyclonal anti-MIF antibodies (**G–I**). (Original magnification × 200.)

weeks after the vaccination; these elevated levels were maintained for at least another 6 weeks (Figure 4A). The clinical severity of autoimmune arthritis in the animals was determined by estimating the arthritis score and the degree of hind paw swelling. The percentage of arthritic mice at the indicated time points was also determined.

Twelve weeks after immunization, the percentage of arthritic mice among animals vaccinated with MIF/TTX was reduced to 20%, compared with 100% of mice receiving saline and 80% of mice immunized with pCAGGS (Figure 4B). Mice vaccinated with MIF/TTX also had significantly lower arthritis scores at 6, 8, and 12 weeks after the vaccination (Figure 4C). The mean paw thickness of the MIF/TTX-vaccinated animals was also significantly lower at 6, 8, and 12 weeks after vaccination compared with that of the pCAGGS-vaccinated mice (Figure 4D). At week 16 after vaccination, histologic examination of the affected ankle joints from saline-treated IL-1Ra–knockout mice revealed severe synovitis, pannus formation, cartilage/bone erosion, and positive immunostaining for MIF in the synovium and

pannus (Figures 5A, D, and G). The affected ankle joints from pCAGGS-vaccinated mice also showed severe synovitis, pannus formation, cartilage/bone erosion, and positive immunostaining for MIF within the synovium and pannus (Figures 5B, E, and H). In contrast, the affected ankle joints from MIF/TTX-vaccinated mice showed only very mild synovitis, cartilage/bone erosion, loss of Safranin O staining of the cartilage, and immunostaining for MIF (Figures 5C, F, and I).

DISCUSSION

In this study, we have shown that active vaccination against MIF could be a novel approach for the treatment of RA and, potentially, other autoimmune disorders as well. It is well known that RA is associated with the abnormally persistent production of TNFα and other proinflammatory cytokines, including interleukin-6 (IL-6), IL-8, and IL-1 (22), in inflamed joint tissue. We focused on MIF as a therapeutic target for RA for the following reasons. First, MIF up-regulates TNFα production by macrophages (2). Second, MIF-deficient mice generate lower amounts of inflammatory cytokines such as TNFα in response to LPS stimulation (23). Third, medium conditioned by cultured rheumatoid synovial fibroblasts induces peripheral blood mononuclear cells to release TNFα; this effect is blocked by anti-MIF antibodies (24). These observations indicate that MIF may be a key upstream regulator of synovial inflammation in RA (24). Thus, suppressing MIF activity may be a more effective manner of treating RA than is suppression of other inflammatory cytokines.

The pathogenesis of the CAIA model may differ somewhat from that of RA in that type II collagen–specific T cells are unlikely to be involved in CAIA; moreover, the initiation of CAIA also requires injection with LPS. However, this experimental model of arthritis has many advantages, namely, this model can cause arthritis with 100% probability in many strains of mice irrespective of their major histocompatibility complex type and within a short period of time (18). Moreover, it has been reported that MIF plays an important role in the pathogenesis of the CAIA model (7,25). However, this model may not be the best one for evaluating the therapeutic effect of MIF DNA vaccination over a long period, because CAIA lasts, at most, 3–4 weeks, which is too short a time period for such an evaluation.

IL-1Ra is an endogenous inhibitor of IL-1, and polyarthritis spontaneously develops in IL-1Ra–knockout mice on the BALB/c background, starting at 5 weeks of age. By 12 weeks of age, almost all mice have affected joints (19). The histopathologic features of the lesions closely resembles those in human RA, because marked synovial and periarticular inflammation and articular erosion caused by invasion of granulation tissues are observed. In this model, excess IL-1 signaling due to the lack of IL-1Ra induces T cell–mediated autoimmunity that results in joint-specific inflammation and bone destruction. Therefore, this model, which is characterized by long disease duration, may be suitable for evaluating over a long period of time the prophylactic effect of a particular approach. Consequently, we investigated the effect of MIF/TTX DNA vaccination on the arthritis in this murine model. Our experiments revealed that a single vaccination with MIF/TTX DNA was sufficient to suppress the incidence and severity of arthritis for at least 12 weeks.

How neutralization of MIF suppresses the development of arthritis in IL-Ra–knockout mice, which is caused by excess IL-1 signaling, remains to be elucidated. Horai et al (19,26) reported that the joints of IL-1Ra–knockout animals have high levels of proinflammatory cytokines such as IL-1β, IL-6, and TNFα, and that inhibiting TNFα function effectively suppresses the development of arthritis in these animals. This suggests that a proinflammatory cytokine network promotes the development of this autoimmune arthritis. Thus, it is possible that MIF, which is known to up-regulate the production of TNFα (3,23,24), may be a prominent upstream component of this network. This hypothesis will need to be tested in additional studies.

The Th cell–modified vaccine approach we used in the current study demonstrates the therapeutic potential of vaccines that generate immune responses against pathogenic self proteins. By incorporating a promiscuous foreign Th cell epitope into self proteins, the immunologic tolerance to self proteins can be bypassed (27–29). DNA vaccines represent a novel means of expressing antigens in vivo that will generate both humoral and cell-mediated immune responses, and the efficacy of DNA vaccines in preclinical animal models has been well documented (30). DNA vaccines have an advantage over recombinant protein vaccines in that the construction and purification of vectors for DNA vaccination are relatively simple. This approach is thus likely to increase the speed and decrease the effort required to develop novel protein vaccines. Moreover, this approach is useful for rapidly screening potential protein immunogens.

Naked cDNA encoding CC chemokines without

a Th cell epitope has been shown to elicit autoantibodies that effectively prevent the development of experimental adjuvant-induced encephalitis (31). The finding that autoantibodies could be generated without the help of a Th cell epitope may be related to the fact that oligonucleotide sequences in the plasmid, such as unmethylated CpG motifs, have been shown to be able to act as immune adjuvant, thereby accelerating antigen-specific immune responses (32). However, Hertz et al (33) reported that unmodified wild-type murine IL-5 cDNA failed to elicit antibodies, which is consistent with the inability of wild-type mMIF cDNA to elicit autoantibodies in the current study.

Thus, the proper selection of a Th cell epitope and its insertion into the appropriate sites of the cDNA may be the key to the successful design of an effective DNA vaccine. Moreover, DNA delivery and DNA vaccine potency may be enhanced by electroporation. Supporting this possibility is the study by Selby et al (34), who reported that mice injected intramuscularly with a plasmid showed a 7.3-fold increase in luciferase expression and 8- to 20-fold enhanced antibody titers when they had also been subjected to electroporation at the time of immunization.

Active immunization with the MIF/TTX DNA vaccine reduced the symptoms of CAIA to the same extent as did therapeutically injected anti-mMIF monoclonal antibodies (7). Our preliminary safety studies, in which we monitored organ weights and the general histologic features of selected tissue, including the liver, kidney, and skin, did not reveal differences between unvaccinated and MIF/TTX DNA-vaccinated mice (data not shown). Similarly, significant differences in the wound-healing ability of mice in the 2 groups were not detected (data not shown). Additional safety studies, including hematologic examinations, are under way.

In conclusion, administration of Th cell–modified MIF DNA is a cost-effective, potentially prophylactic method of vaccination that can inhibit CAIA and spontaneous arthritis in IL-1Ra–knockout mice. Thus, active vaccination against MIF is a novel approach to the treatment of RA and possibly other autoimmune diseases as well.

AUTHOR CONTRIBUTIONS

Dr. Koyama had full access to all of the data in the study and takes responsibility for the integrity of the data and the accuracy of the data analysis.

Study design. Drs. Onodera, Nishihira, and Koyama.

Acquisition of data. Drs. Onodera, Oshima, and Iwakura, Mr. Matsuda, and Dr. Koyama.

Analysis and interpretation of data. Drs. Onodera and Koyama.

Manuscript preparation. Drs. Onodera, Yasuda, Minami, and Koyama.

Statistical analysis. Drs. Onodera and Tohyama.

REFERENCES

1. Morand EF. New therapeutic target in inflammatory disease: macrophage migration inhibitory factor. Intern Med J 2005;35: 419–26.
2. Onodera S, Tanji H, Suzuki K, Kaneda K, Mizue Y, Sagawa A, et al. High expression of macrophage migration inhibitory factor in the synovial tissues of rheumatoid joints. Cytokine 1999;11:163–7.
3. Bernhagen J, Mitchell RA, Calandra T, Voelter W, Cerami A, Bucala R. Purification, bioactivity, and secondary structure analysis of mouse and human macrophage migration inhibitory factor (MIF). Biochemistry 1994;33:14144–55.
4. Onodera S, Kaneda K, Mizue Y, Koyama Y, Fujinaga M, Nishihira J. Macrophage migration inhibitory factor (MIF) up-regulates expression of matrix metalloproteinases in synovial fibroblasts of rheumatoid arthritis. J Biol Chem 2000;275:444–50.
5. Sampey AV, Hall PH, Mitchell RA, Metz CN, Morand EF. Regulation of synoviocyte phospholipase A_2 and cyclooxygenase 2 by macrophage migration inhibitory factor. Arthritis Rheum 2001; 44:1273–80.
6. Leech M, Lacey D, Xue JR, Santos L, Hutchinson P, Wolvetang E, et al. Regulation of p53 by macrophage migration inhibitory factor in inflammatory arthritis. Arthritis Rheum 2003;48:1881–9.
7. Ichiyama H, Onodera S, Nishihira J, Ishibashi T, Nakayama T, Minami A, et al. Inhibition of joint inflammation and destruction induced by anti-type II collagen antibody/lipopolysaccharide (LPS)-induced arthritis in mice due to deletion of macrophage migration inhibitory factor (MIF). Cytokine 2004;26:187–94.
8. Morand EF, Leech M, Wedon H, Metz C, Bucala R, Smith MD. Macrophage migration inhibitory factor in rheumatoid arthritis: clinical correlations. Rheumatology 2002;41:558–62.
9. Baugh JA, Chitnis S, Donnely SC, Monteiro J, Lin X, Plant BJ, et al. A functional promoter polymorphism in the macrophage migration inhibitory factor (MIF) gene associated with disease severity in rheumatoid arthritis. Genes Immun 2002;3:170–6.
10. Mikulowska A, Metz CN, Bucala R, Holmdahl R. Macrophage migration inhibitory factor is involved in the pathomechanism of collagen type-II induced arthritis in mice. J Immunol 1997;158: 5514–7.
11. Leech M, Metz CN, Santos L, Peng T, Holdsworth SR, Bucala R, et al. Involvement of macrophage migration inhibitory factor in the evolution of rat adjuvant arthritis. Arthritis Rheum 1998;41: 910–7.
12. Clark M. Antibody humanization: a case of the 'Emperor's new clothes'? Immunol Today 2000;21:397–402.
13. Horai R, Asano M, Sudo K, Kanuka H, Suzuki M, Nishihara M, et al. Production of mice deficient in genes for interleukin (IL)-1α, IL-1β, IL-1α/β, and IL-1 receptor antagonist shows that IL-1β is crucial in turpentine-induced fever development and glucocorticoid secretion. J Exp Med 1998;187:1463–75.
14. Niwa H, Yamamura K, Miyazaki J. Efficient selection for high-expression transfectants with a novel eukaryotic vector. Gene 1991;108:193–200.
15. Panina-Bordignon P, Tan A, Termijtelen A, Demotz S, Corradin G, Lanzavecchia A. Universally immunogenic T cell epitopes: promiscuous binding to human MHC class II and promiscuous recognition by T cells. Eur J Immunol 1989;19:2237–42.

16. Aihara H, Miyazaki J. Gene transfer into muscle by electroporation in vivo. Nature Biotech 1998;16:867–70.
17. Kobayashi S, Nishihira J, Watanabe S, Todo S. Prevention of lethal acute hepatic failure by antimacrophage migration inhibitory factor antibody in mice treated with bacille Calmette-Guerin and lipopolysaccharide. Hepatology 1999;29:1752–9.
18. Terato K, Harper DS, Griffiths MM, Hasty DL, Ye XJ, Cremer MA, et al. Collagen-induced arthritis in mice: synergistic effect of E. coli lipopolysaccharide bypasses epitope specificity in the induction of arthritis with monoclonal antibodies to type II collagen. Autoimmunity 1995; 22:137–47.
19. Horai R, Saijo S, Tanioka H, Nakae S, Sudo K, Okahara A, et al. Development of chronic inflammatory arthropathy resembling rheumatoid arthritis in interleukin 1 receptor antagonist-deficient mice. J Exp Med 2000;191:313–20.
20. Suzuki M, Sugimoto H, Nakagawa A, Tanaka I, Nishihira J, Sakai M. Crystal structure of the macrophage migration inhibitory factor from rat liver. Nature Struct Biol 1996;3:259–66.
21. Spohn G, Schwarz K, Maurer P, Illges H, Rajasekaran N, Choi Y, et al. Protection against osteoporosis by active immunization with TRANCE/RANKL displayed on virus-like particles. J Immunol 2005;175:6211–8.
22. Brennan FM, Chantry D, Jackson A, Maini R, Feldmann M. Inhibitory effect of TNF α antibodies on synovial cell interleukin-1 production in rheumatoid arthritis. Lancet 1989;2:244–7.
23. Bozza M, Satoskar AR, Lin G, Lu B, Humbles AA, Gerard C, et al. Targeted disruption of migration inhibitory factor gene reveals its critical role. J Exp Med 1999;189:341–6.
24. Leech M, Metz C, Hall P, Hutchinson P, Gianis K, Smith M, et al. Macrophage migration inhibitory factor in rheumatoid arthritis: evidence of proinflammatory function and regulation by glucocorticoids. Arthritis Rheum 1999;42:1601–8.
25. Onodera S, Nishihira J, Koyama Y, Majima T, Aoki Y, Ichiyama H, et al. Macrophage migration inhibitory factor up-regulates the expression of interleukin-8 messenger RNA in synovial fibroblasts of rheumatoid arthritis patients: common transcriptional regulatory mechanism between interleukin-8 and interleukin-1β. Arthritis Rheum 2004;50:1437–47.
26. Horai R, Nakajima A, Habiro K, Kotani M, Nakae S, Matsuki T, et al. TNF-α is crucial for the development of autoimmune arthritis in IL-1 receptor antagonist-deficient mice. J Clin Invest 2004;114:1603–11.
27. Dalum I, Jensen MR, Hindersson P, Elsner HI, Mouritsen S. Breaking of B cell tolerance toward a highly conserved self protein. J Immunol 1996;157:4796–804.
28. Dalum I, Jensen MR, Gregorius K, Thomasen CM, Elsner HI, Mouritsen S. Induction of cross-reactive antibodies against a self protein containing a foreign T helper epitope. Mol Immunol 1997;34:1113–20.
29. Dalum I, Butler DM, Jensen MR, Hindersson P, Steinaa L, Waterston AM, et al. Therapeutic antibodies elicited by immunization against TNF-α. Nat Biotechnol 1999;17:666–9.
30. Donnelly JJ, Ulmer JB, Liu MA. DNA vaccines. Life Sci 1997;60: 163–72.
31. Youssef S, Wildbaum G, Maor G, Lanir N, Gour-Lavie A, Grabie N, et al. Long-lasting protective immunity to experimental autoimmune encephalomyelitis following vaccination with naked DNA encoding C-C chemokines. J Immunol 1998;161:3870–9.
32. Klinman DM, Currie D, Gursel I, Verthelyi D. Use of CpG oligodeoxynucleotides as immune adjuvants. Immunol Rev 2004; 99:201–16.
33. Hertz M, Mahalingam S, Dalum I, Klysner S, Mattes J, Neisig A, et al. Active vaccination against IL-5 bypasses immunological tolerance and ameliorates experimental asthma. J Immunol 2001; 167:3792–9.
34. Selby M, Goldbeck C, Pertile T, Walsh R, Ulmer J. Enhancement of DNA vaccine potency by electroporation in vivo. J Biotechnol 2000;83:147–52.

Available online at www.sciencedirect.com
ScienceDirect
Journal of Chromatography B, 853 (2007) 133–137
JOURNAL OF CHROMATOGRAPHY B
www.elsevier.com/locate/chromb

Detection of altered *N*-glycan profiles in whole serum from rheumatoid arthritis patients

Hiroaki Nakagawa[a,*], Megumi Hato[a], Yasuhiro Takegawa[a], Kisaburo Deguchi[a], Hiroki Ito[b], Masahiko Takahata[c], Norimasa Iwasaki[c], Akio Minami[c], Shin-Ichiro Nishimura[a,*]

[a] *Graduate School of Advanced Life Science, Frontier Research Center for Post-Genomic Science and Technology, Hokkaido University, W11 N21, Sapporo 001-0021, Japan*
[b] *Hitachi High-Technologies Company, Hitachinaka 312-8504, Japan*
[c] *Department of Orthopaedic Surgery, Hokkaido University Graduate School of Medicine, Sapporo 060-8638, Japan*

Received 15 January 2007; accepted 5 March 2007
Available online 19 March 2007

Abstract

Altered *N*-glycosylation occurs in many diseases. In rheumatoid arthritis (RA), for example, reduction in galactose residues in IgG and an increase in fucose residues in α1-acid glycoprotein have been observed. To further analyse *N*-glycans in disease, we show *N*-glycan profiling from whole serum employing reversed phase high performance liquid chromatography/negative-ion mode by sonic spray ionization ion trap mass spectrometry with pyridylamination. Profiles from female 15 RA patients and 18 aged-matched healthy women were compared. The most significant change seen in RA was decreased levels of mono-galactosyl bi-antennary *N*-glycans, in agreement with the previous reports regarding IgG. We also show previously unreported differences between isomers and increased tri-antennary oligosaccharides. These results indicate that LC–MS analysis of whole serum *N*-glycans can identify *N*-glycan alterations in RA and that this is a promising method both for studies of RA mechanisms and diagnosis.

Keywords: *N*-glycan; Serum; Rheumatoid arthritis; LC–MS

1. Introduction

N-Glycans are attached to nascent polypeptides in the endoplasmic reticulum and modified in the Golgi apparatus by numerous glycosidases and glycosyltransferases. *N*-glycans function as tags for protein localization and clearance, and their profiles, structures, and ratios are affected by several physiological conditions.

One particularly dramatic oligosaccharide change associated with disease is reduced galactose in IgG *N*-glycans seen in patients with rheumatoid arthritis (RA) [1]. Fucosylation of IgG [2] and *N*-glycan microheterogeneities in α1-acid glycoproteins (AGP) [3,4], transferrin [5], haptoglobin [6], α2-macrogloblin [7], and other plasma proteins [8] have also been reported in RA, although how alterations are associated with symptoms is not known [9]. Several methods have been applied to the analysis of IgG *N*-glycans, such as reversed phase-high performance liquid chromatography (RP-HPLC), liquid chromatography–mass spectrometry (LC–MS), lectin analysis, and high pH anion exchange chromatography-pulsed amperometric detection (HPAEC-PAD) [10].

Here we compared profiles of whole serum *N*-glycans from RA patients and healthy women. RP-HPLC using fluorescence-tagged *N*-glycans is a useful method to detect alteration of core-fucosylated bi-antennary oligosaccharides including isomers in IgG. However, tri-antennary *N*-glycans which bind other serum glycoproteins overlap with core-fucosyl and mono-galactosyl bi-antennary glycans in RP-HPLC analysis [11]. Analysis of *N*-glycans by mass spectrometry (MS) is often complicated by low quantitative reliability. Sonic spray ionization ion trap mass spectrometry (SSI-IT/MS) ionizes mildly with nitrogen gas flow [12] and is applicable to quantitative analysis of neutral and sialic oligosaccharides in the negative ion mode [13,14]. Thus we

* Corresponding authors. Tel.: +81 11 706 9031; fax: +81 706 9032.
E-mail addresses: nakagawa@glyco.sci.hokudai.ac.jp (H. Nakagawa), shin@glyco.sci.hokudai.ac.jp (S.-I. Nishimura).

1570-0232/$ – see front matter © 2007 Elsevier B.V. All rights reserved.
doi:10.1016/j.jchromb.2007.03.003

combined SSI-IT and MS in order to compare *N*-glycan profiles from whole sera of healthy women and female RA patients.

2. Experimental

2.1. Chemicals

Trypsin and chymotrypsin were purchased from Sigma (Sigma–Aldrich, St Louis, MO). Peptide-*N*-glycosidase F (PNGase F, recombinant) was purchased from Roche Diagnosis (Basel, Switzerland). The following materials were purchased from the sources indicated: Pronase, Calbiochem (Merck KGaA, Darmstadt, Germany); Sephadex G-15, Amersham Biosciences (Piscataway, NJ); Bio-Gel P-4 (200–400 mesh), Bio-Rad (Hercules, CA); sodium cyanoborohydride, Sigma–Aldrich (St Louis, MO); and 2-aminopyridine, Wako Pure Chemical Industries (Osaka, Japan).

2.2. Preparation of serum N-glycans

Human serum samples were obtained from the Hospital of Hokkaido University with written informed consent of all subjects following ethical standards of Hokkaido University. Groups of 15 female RA patients and 18 female age-matched healthy controls were median aged 55 and 53 years, ranging from 50–58 and 45–64 years, respectively. One patient was stage 3 and the rest were stage 4, according to staging of Steinbrocker et al. [15].

Sera were treated as described [11,16] with minor modifications. Each 50 μl aliquot of sera was heated to 90 °C for 15 min and incubated with 35 μg each of trypsin and chymotrypsin for 37 °C for 16 h. Proteases were inactivated by heating, *N*-glycans were released by PNGase F, and peptides were then digested by pronase. *N*-Glycans were purified by gel-filtration using Bio-Gel P-4 (1 cm × 38 cm, H_2O) and tagged fluorescently by pyridylamination (PA) [17,18]. PA-glycans were purified by another gel filtration on a Sephadex G-15 column with 10 mM ammonium bicarbonate. To release sialic acid, collected PA-glycan fractions were heated to 90 °C for 1 h at pH 2.0 with HCl. Neutral PA-glycans were further purified using HPLC (Hitachi L-7000 HPLC system, Hitachi High-Technologies Co., Tokyo, Japan) on an amide column (TSKgel Amide-80, 4.6 × 250 mm, TOSOH, Tokyo, Japan) at a flow rate of 1.0 ml per minute at 40 °C with solvent A (3% (v/v) acetic acid - triethylamine (pH 7.3)/acetonitrile 35:65) and solvent B (3% (v/v) acetic acid - triethylamine (pH 7.3)/acetonitrile 65:35). The column was initially equilibrated with solvent A only, and the elution was changed 7 min after injection to solvent B only. The PA-oligosaccharide mixture eluted as one peak was detected by fluorescence (excitation and emission wavelengths of 320 nm and 400 nm, respectively). Separated *N*-glycans were then analyzed by LC–MS.

2.3. RP-HPLC/SSI-IT/MS analysis

Oligosaccharides were separated and their mass chromatograms monitored using the L-7000 HPLC system combined with an M-8000 3DQ ion trap-equipped SSI interface (Hitachi High-Technologies). Separations were on a reversed phase column, Develosil C30-UG (2 mm × 150 mm, Nomura Chem., Seto, Japan), at 40 °C and in buffer containing 0.2 ml/min of 1 mM ammonium acetate, pH 4.3, with a linear gradient of acetonitrile (from 1.3% at 0 min to 6.0% at 70 min). MS conditions were as follows: desolvation temperature, 260 °C; nitrogen gas pressure, 400 kPa; capillary voltage, 0 V; drift voltage, 80 V; scan range, *m/z* 200–2000; and scan time, 500 ms.

Data are presented as means ± SD. Statistical significance was determined using the two-tailed Student's *t* test.

3. Results

Chromatograms of serum *N*-glycans were monitored by fluorescence and base ion chromatography by mass spectrometry (Fig. 1). *N*-Glycan structures and linkages are shown in Fig. 1(C). The oligosaccharide numbering system is according to Takahashi et. al. [16], which is a system suitable to distinguish isomers. As an example of numbering, numbers in the range of one hundred indicate the number of branches, the second number indicates the presence of core fucose, and the number before the dot bisecting GlcNAc and

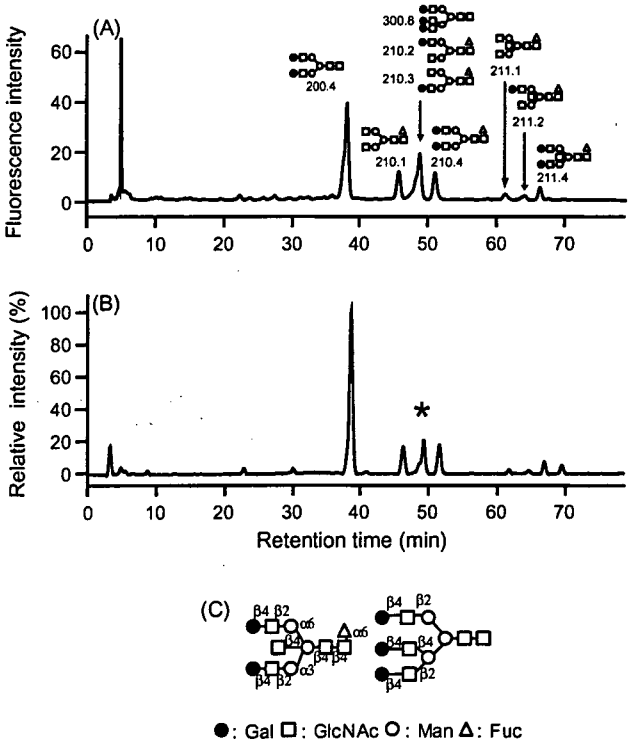

Fig. 1. Chromatograms of serum *N*-glycans on a reversed phase column using HPLC. A, fluorescence detection: Ex = 320 nm and Em = 400 nm. Elution conditions were as follows: column, Develosil C30-UG 2 × 150 mm; temperature, 40 °C; solvent, 1 mM ammonium acetate pH4.3 with a linear gradient of acetonitrile 1.3 to 6.0% in 70 min. B, base ion chromatogram of *m/z* 200–2000 in negative mode by SSI-IT/MS. MS is connected after the fluorescence detector. The asterisk indicates a peak including three major oligosaccharides: 210.2, 200.3, and 300.8. C, *N*-glycan linkages shown in Fig. 1A. Details of this numbering system and list are presented in reference [16] and at http://www.glycoanalysis.info/index.html.

Table 1
Oligosaccharides with mass numbers and ion types analyzed in this study

Oligosaccharide	m/z	Ion type	Elution time (min)
200.4	859	$[M-2H]^{2-}$	36.8–39.2
	878	$[M-H+Cl]^{2-}$	36.8–39.3
	1718	$[M-H]^{-}$	37.1–39.2
210.1	770	$[M-2H]^{2-}$	45.2–47.0
	1540	$[M-H]^{-}$	45.1–47.1
210.2	851	$[M-2H]^{2-}$	47.4–48.7
	870	$[M-H+Cl]^{2-}$	47.6–48.7
	1702	$[M-H]^{-}$	47.5–48.7
210.3	851	$[M-2H]^{2-}$	48.7–50.0
	870	$[M-H+Cl]^{2-}$	48.7–50.1
	1702	$[M-H]^{-}$	48.7–49.9
300.8	1042	$[M-2H]^{2-}$	47.7–49.8
	1061	$[M-H+Cl]^{2-}$	47.7–49.9
210.4	932	$[M-2H]^{2-}$	50.4–52.2
	951	$[M-H+Cl]^{2-}$	50.4–52.5
	1864	$[M-H]^{-}$	50.4–51.9
211.1	871	$[M-2H]^{2-}$	60.4–62.8
	1743	$[M-H]^{-}$	60.6–62.2
211.2	952	$[M-2H]^{2-}$	63.0–65.7
211.4	1034	$[M-2H]^{2-}$	65.6–67.6
	1052	$[M-H+Cl]^{2-}$	65.5–67.8

For example, 300.8 was detected at *m/z*1042 and corresponds to $[M-2H]^{2-}$ ion, and 1060 corresponds to $[H-H+Cl]^{2-}$ ions. The mass chromatogram of 1042 (±1) such as that seen in Fig. 2B-2 was recognized between 47.7–49.8 min.

to the right of the period represents a serial number. A list of numbers and structures is presented in reference [16] and on the website http://www.glycoanalysis.info/index.html. Each oligosaccharide was detected with several ions; *N*-glycans identified and types of ions are shown in Table 1. Amounts of *N*-glycans were calculated based on areas of their mass chromatograms. Three *N*-glycans overlapped at the point marked by an asterisk in Fig. 1 [13]. Mass spectra of this peak included the following signals: 851, 870 and 1702 were from 210.2 or 210.3, which are isomers of fucosylated mono-galactosyl bi-antennary oligosaccharides, and 1042 and 1061 were from the tri-antennary oligosaccharide 300.8 (Fig. 2A). These *N*-glycans could not be distinguished by fluorescence analysis. On the other hand, mass chromatograms separated these species, and areas of these *N*-glycans were determined quantitatively (Fig. 2B). In Fig. 2B-1, the mass chromatogram of 851 *m/z* showed separation of isomers 210.2 and 210.3 on RP-HPLC, and only 300.8 appeared in mass chromatograms of 1042 (Fig. 2B-2).

A comparison of RA patients and healthy women is shown in Fig. 3. A previous study showed that the mass chromatogram area was correlated with the chromatography area by fluorescence [14]. The ratio of a specific oligosaccharide is calculated on the mass chromatogram from the area of the peak of that glycan relative to the total area of 9 glycans, which is defined as 100%. In RA patients, 210.3, an isomer of fucosylated mono-galactosyl bi-antennary oligosaccharide, was significantly decreased ($P<0.001$), as was the 210.2 isomer ($P<0.01$). On the other hand, the tri-antennary *N*-glycan 300.8 ($P<0.01$) was increased in RA relative to control subjects.

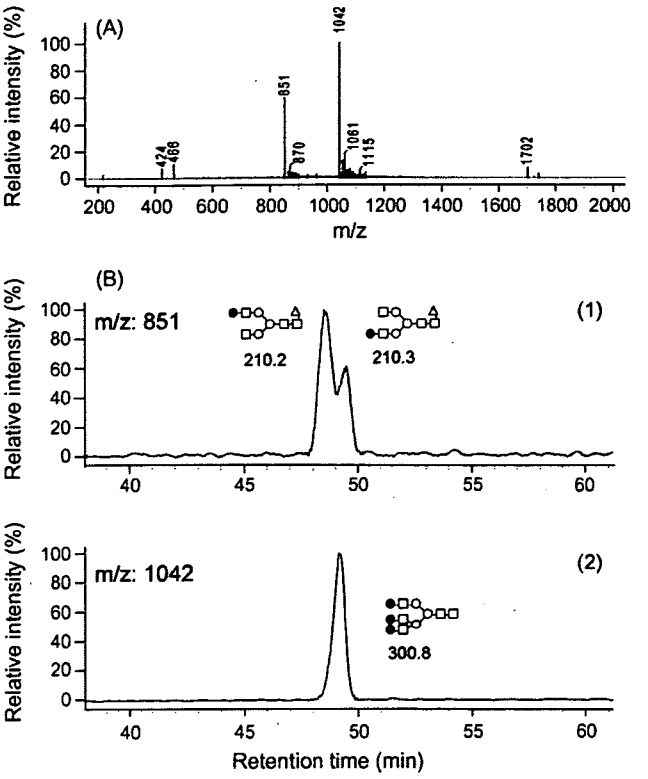

Fig. 2. Analysis of the peak marked by an asterisk in Fig. 1B using mass spectrometry. A, mass spectrum of the peaks. Signals *m/z* 1042 and 1061 were from 300.8, and 851, 870 and 1702 were ions of 210.2 and 210.3. B-1; separated isomers 210.2 and 210.3 detected by mass chromatogram of *m/z* 851 ±1 correspond to $[M-2H]^{2-}$ ions of these isomers. B-2; Mass chromatogram of *m/z* = 1042 ±1 corresponding to the $[M-2H]^{2-}$ ion of tri-antennary oligosaccharide, 300.8.

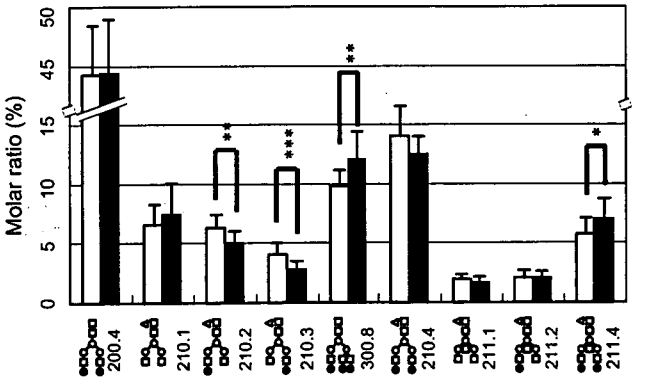

Fig. 3. Comparison of oligosaccharide ratios between 15 RA patients and 18 age-matched healthy women. A previous study showed that the mass chromatogram area was correlated with the chromatography area by fluorescence [14]. The ratio of a specific oligosaccharide is calculated on the mass chromatogram from the area of the peak of that glycan relative to the total area of 9 glycans, which is defined as 100%. Error bars show SD. Asterisk shows statistical significance using two-tailed Student's *t* test; $*P<0.05$; $**P<0.01$ and $***P<0.001$. *P* values of 210.2, 210.3, 300.8 and 211.4 are 0.00599, 0.00019, 0.00493 and 0.04637 respectively.

4. Discussion

Twenty years have passed since the finding that IgG *N*-glycans are altered in RA. Such *N*-glycan alterations have also been reported also other serum proteins; thus alterations in serum

N-glycans in RA are anticipated but have not yet been reported because of technical difficulties. Here, we undertook glycomic analysis of whole sera using RP-HPLC/SSI-IT MS and succeeded in showing such alterations in RA patients.

In previous comparisons of serum *N*-glycans from RA to age-matched healthy women, galactose residues were reportedly decreased [1,10]. Here we report two new findings. First, decreases in the mono-galactosyl oligosaccharide isomer 210.3 were more significant than those of another isomer, 210.2. These isomers differ in a branch that binds galactose, and it has been suggested that their ratio reflects a difference between IgG subclasses [19,20]. IgG subclasses have different properties and their activities depend on the type of antigen [21]. Thus oligosaccharide alterations associated with IgG subclass may be critical.

Another altered tri-antennary oligosaccharide may be derived from AGP, a major serum glycoprotein. AGP increases in RA, and alteration in its glycans detected by lectin binding has been reported [3]. Another major glycoprotein, transferrin, accounts for a small proportion of the tri-antennary oligosaccharides found in healthy adults [22], and IgG and haptoglobin reportedly exhibit bi-antennary [23,24] rather than tri-antennary oligosaccharides. However, alteration in AGP *N*-glycans in RA is reported to involve only fucosylation, and proteomic analysis of serum in RA using 2-D PAGE and lectins shows changes in IgG, haptoglobin, and two unknown glycoproteins, but not in AGP [8]. Thus, the observed increase in tri-antennary oligosaccharides may occur in glycoproteins other than AGP, supporting the importance of analyzing whole serum *N*-glycans rather than just oligosaccharides on purified glycoproteins. Further analysis, such as quantitative glyco-proteomics analysis, is required. Another reported alteration in RA, an increase in fucosylated tri-antennary species, was not analyzed in this study, possibly because it was a minor peak [11]. In Fig. 2A, the *m/z* 1115 signal coincides with fucosylated tri-antennary oligosaccharide, but signals from some samples were too weak to be detected in mass chromatograms. Following improvements in sensitivity or resolution, the method utilized here is applicable to other disease or oligosaccharide alterations. SSI-IT/MS can also be used to analyze sialyl oligosaccharides and distinguish isomers using MS^n [12,13]; thus a combination of SSI-IT/MS and RP-HPLC should be widely applicable to *N*-glycan analysis.

Weak acid lysis for sialic acids were used in this and the previous studies [19,20,23]. Conditions are different with each reference, because the result may differ by tube material and size, sample volume and heating unit using which affect heating. We confirm the conditions, at 90 °C, pH 2.0 with HCl, for 60 min using our tube and heater.

In conclusion, glycomics of whole serum using RP-HPLC/SSI-IT MS showed decreased mono-galactosyl bi-antennary oligosaccharides in RA patients, as reported previously. We also report two new findings: a difference in mono-galactosyl oligosaccharide isomers in RA patients and increased levels of tri-antennary *N*-glycans. Glycomics analyses can provide valuable information relevant to disease and should aid the progress of the research about disease mechanisms. Changes in IgG glycan profiles are useful for early stage diagnosis of RA [25]. This method does not require IgG purification and can provide information about other serum proteins. It also could facilitate diagnosis, because early stage diagnosis, which is not yet achievable, is critical for treatment [26,27]. Future studies should focus on well designed, large scale groups including subjects of various ages, sex, disease progression, and values of serum proteins including IgG subclass.

Acknowledgements

This work was supported in part by SENTAN from the Japan Science and Technology Agency and the National Project on Functional Glycoconjugate Research Aimed at Developing New Industry from the Ministry of Education, Culture, Sports, Science and Technology of Japan. We thank Ms Kazue Okada very much for technical assistance.

References

[1] R.B. Parekh, R.A. Dwek, B.J. Sutton, D.L. Fernades, A. Leung, D. Stanworth, T.W. Rademacher, T. Mizuochi, T. Taniguchi, K. Matsuta, F. Takeuchi, Y. Nagano, T. Miyamoto, A. Kobata, Nature 316 (1985) 452.
[2] I. Gornik, G. Marvic, J. Dumic, M. Flögel, G. Lauc, Clin. Biochem. 32 (1999) 605.
[3] A. Mackiewicz, T. Pawlowski, A. Mackiewicz-Pawlowska, K. Wiktorowicz, S. Mackiewicz, Clin. Chim. Acta 163 (1987) 185.
[4] S.K. Moule, M. Peak, S. Thompson, G.A. Turner, Clin. Chim. Acta 166 (1987) 177.
[5] R.A. Feelders, G. Vreugdenhil, G. de Jong, A.J.G. Swaak, H.G. van Eijk, Rheumatol. Int. 12 (1992) 195.
[6] S. Thompson, C.A. Kelly, I.D. Griffiths, G.A. Turner, Clin. Chim. Acta 184 (1989) 251.
[7] L. Saso, B. Silvestrini, A. Guglielmotti, R. Lahita, C.Y. Cheng, Inflammation 17 (1993) 465.
[8] S.K. Raghav, B. Gupta, C. Agrawal, A. Saroha, R.H. Das, V.P. Chaturavedi, H.R. Das, Glycoconjugate J. 23 (2006) 167.
[9] J.S. Axford, Biochem. Biophys. Acta 1455 (1999) 219.
[10] F.H. Routier, E.F. Hounsell, P.M. Rudd, N. Takahashi, A. Bond, F.C. Hay, A. Alavi, J.S. Axford, R. Jefferis, J. Immunol. Methods 213 (1998) 113.
[11] H. Nakagawa, Y. Kawamura, K. Kato, I. Shimada, Y. Arata, N. Takahashi, Anal. Biochem. 226 (1995) 130.
[12] A. Hirabayashi, M. Sakairi, H. Koizumi, Anal. Chem. 66 (1994) 4557.
[13] Y. Takegawa, K. Deguchi, S. Ito, S. Yoshioka, A. Sano, K. Yoshinari, K. Kobayashi, H. Nakagawa, K. Monde, S.-I. Nishimura, Anal. Chem. 76 (2004) 7294.
[14] Y. Takegawa, K. Deguchi, S. Ito, S. Yoshioka, H. Nakagawa, S.-I. Nishimura, Anal. Chem. 77 (2005) 2097.
[15] O. Steinbrocker, C.H. Traeger, R.C. Batterman, J. Am. Med. Assoc. 140 (1949) 659.
[16] N. Takahashi, N. Tomiya, in: N. Takahashi, T. Muramatsu (Eds.), Handbook of Endoglycosidases and Glycoamidases, CRC Press, Boca Raton FL, 1992, p. 199.
[17] S. Hase, T. Ikenaka, Y. Matsushima, Biochem. Biophys. Res. Commun. 85 (1978) 257.
[18] S. Yamamoto, S. Hase, S. Fukuda, O. Sano, T. Ikenaka, J. Biochem. 105 (1989) 547.
[19] R. Jefferis, J. Lund, H. Mizutani, H. Nakagawa, Y. Kawazoe, Y. Arata, N. Takahashi, Biochem. J. 268 (1990) 529.
[20] M. Tandai, T. Endo, S. Sasaki, Y. Masuho, N. Kochibe, A. Kobata, Arch. Biochem. Biophys. 291 (1991) 339.
[21] G.A. Maguir, D.S. Kumararatne, H.J. Joyce, Ann. Clin. Biochem. 39 (2002) 374.

[22] K. Yamashita, N. Koide, T. Endo, Y. Iwaki, A. Kobata, J. Biol. Chem. 264 (1989) 2415.
[23] S. Thompson, E. Dargan, I.D. Griffiths, C.A. Kelly, G.A. Turner, Clin. Chim. Acta 220 (1993) 107.
[24] M.T. Goodarzi, G.A. Turner, Glycoconjugate J. 15 (1998) 469.
[25] M. Watoson, P.M. Rudd, M. Bland, R.A. Dwek, J.S. Axford, Arthritis Rheum. 42 (1999) 1682.
[26] H. Visser, Best Pract. Res. Clin. Rheumatol. 19 (2005) 55.
[27] J. Morel, B. Combe, Best Pract. Res. Clin. Rheumatol. 19 (2005) 137.

ELSEVIER

Bone 41 (2007) 77–86

BONE

www.elsevier.com/locate/bone

Sialylation of cell surface glycoconjugates is essential for osteoclastogenesis

Masahiko Takahata [a,*], Norimasa Iwasaki [a], Hiroaki Nakagawa [b], Yuichiro Abe [a], Takuya Watanabe [b], Manabu Ito [a], Tokifumi Majima [a], Akio Minami [a]

[a] *Department of Orthopaedic Surgery, Hokkaido University Graduate School of Medicine, Kita-15 Nishi-7, Kita-ku, Sapporo 060-8638, Japan*
[b] *Division of Biological Sciences, Graduate School of Science, Hokkaido University, Japan*

Received 17 February 2007; revised 17 March 2007; accepted 20 March 2007
Available online 5 April 2007

Abstract

Sialic acid, which is located at the end of the carbohydrate moiety of cell surface glycoconjugates, is involved in many biologic responses, such as intercellular reactions and virus–cell fusion, especially in hematopoietic cells. Here we provide experimental evidence that the sialic acid of cell surface glycoconjugates has a role in osteoclast differentiation. Lectin histochemical study demonstrated the existence of both alpha (2,3)-linked-sialic acid and alpha (2,6)-linked-sialic acid in mouse bone marrow-derived macrophages and in the RAW264.7 macrophage cell line, which are osteoclast precursors. Flow cytometric analysis of surface lectin staining revealed the kinetics of these sialic acids during osteoclastogenesis: alpha (2,3)-linked-sialic acid was abundantly expressed throughout osteoclastogenesis, whereas alpha (2,6)-linked-sialic acid levels declined at the terminal stage of osteoclast differentiation. To investigate the role of sialic acid in osteoclast differentiation, we performed an osteoclastogenesis assay with or without exogenous sialidase treatment. Desialylated cells formed TRAP-positive mononuclear cells, but did not become multinuclear cells despite the normal expression of osteoclast markers such as cathepsin K, integrin β3, and nuclear factor-ATc1. Flow cytometric analysis also demonstrated that exogenous sialidase effectively removed alpha (2,6)-linked-sialic acid, but only slightly changed the alpha (2,3)-linked-sialic acid content, suggesting that alpha (2,6)-linked-sialic acid might be involved in osteoclast differentiation. Findings from knockdown analysis using small interfering RNA oligonucleotides against alpha 2,6-sialyltransferase support this idea: alpha (2,6)-linked-sialic acid-deficient cells markedly inhibit the formation of multinuclear osteoclasts. Our findings suggest that alpha (2,6)-linked-sialic acid of cell surface glycoconjugates has a role in osteoclast differentiation, possibly via its role in the cell–cell fusion process.

Keywords: Osteoclast; Cell fusion; Sialic acid; Glycoconjugate; Sialidase

Introduction

Osteoclasts are bone-resorbing cells that have a pivotal role in bone remodeling. Osteoclasts are differentiated from hematopoietic precursors of the monocyte/macrophage lineage and form multinuclear giant cells via cell–cell fusion [2,35]. Multinucleation is thought to be an essential step in the structural and functional differentiation of osteoclasts, because mononuclear osteoclasts cannot efficiently resorb bone. Recent studies revealed candidate molecules involved in osteoclast fusion: E-cadherin [17], macrophage fusion receptor [37], terminal high mannose type oligosaccharide-mannose receptor [22], ADAM9 [25], CD98 [33], $P2X_7$ receptor [6], CD9 [11], and dendritic cell-specific transmembrane protein [15,38]. The complex mechanisms that govern cell–cell fusion in osteoclast differentiation, however, are not fully understood.

It is well established that cell fusion is a biologically and pathophysiologically important event in vivo and occurs not only in osteoclasts, but also among foreign body giant cells [18,24], myoblasts [5], sperm and egg [9,26], and virus and cells [32,23]. Among these, cell surface sialic acid is implicated in some fusion mechanisms. The best known fusion mechanism is the sialic acid recognition and binding mechanism in virus–cell fusion. In parainfluenza virus–cell fusion, sialic acid residues of the uninfected host cell surface are recognized by the hemagglutinin of the virus protein, and interactions between these molecules mediate fusion of virus

* Corresponding author. Fax: +81 11 706 6054.
E-mail address: takamasa@med.hokudai.ac.jp (M. Takahata).

8756-3282/$ - see front matter © 2007 Elsevier Inc. All rights reserved.
doi:10.1016/j.bone.2007.03.016